CALCULATIONS OF VOLTAGES FOR MAGNETO-TELLURIC MODELLING OF A REGION WITH NEAR-SURFACE INHOMOGENEITIES

by

HELENA EVA POLL

B.Sc., University of Guelph, 1985

A THESIS SUBMITTED IN PARTIAL FULFILLMENT

OF THE REQUIREMENTS FOR THE DEGREE OF

MASTER OF SCIENCE

in the Department

of

Physics

ACCEPTED
FACULTY OF GRADUATE STUDIES
[redacted]
DEAN
DATE June 27, 1987

We accept this thesis as conforming

to the required standard

[redacted]

J.T. Weaver

[redacted]

R.E. Horita

[redacted]

V.K. Bhargava

[redacted]

A. Zielinski

ABSTRACT

Supervisor: Professor J.T. Weaver

In the magneto-telluric method, the electric field measurements are obtained by recording the voltages between grounded electrodes and dividing by their separation distances. Such a procedure gives the true value of the electric field only if it is uniform between the electrodes. In regions of near surface inhomogeneities this condition is not fulfilled and in extreme cases each electrode may be in contact with surface material of different resistivity.

In this thesis a method is developed to modify an existing two-dimensional finite difference program so that voltages rather than electric fields are calculated at each node of the numerical grid in the B-polarization model. The numerical results are checked against the exact analytical expressions for voltage obtained for the control model of Weaver, Le Quang, and Fischer (1985). Both the analytical and numerical expressions for voltage are presented in a form suitable for programming and a method for dealing with an electrode profile that is not perpendicular to the strike is

developed. (A listing of the Fortran programs for the analytic calculations and the Fortran subroutines for the numerical calculations are included in the appendix.)

Finally real data obtained over the Gloucester fault in Canada are compared with results given by finite difference modelling based both on voltage calculations and on the more traditional electric field calculations. Although neither numerical method is in remarkably close agreement with the real data the voltage result is a better approximation to the observed behavior of the measured electric field.

Some errors inherent in the magneto-telluric studies of such regions are discussed notably that of a spurious electric field parallel to the fault which arises in voltage calculations when the electrode profile is not perpendicular to the fault.

[redacted]

J.T. Weaver R.E. Horita

[redacted]

V.K Bhargava A. Zielinski

TABLE OF CONTENTS

Page

ABSTRACT..... ii

LIST OF TABLES..... vi

LIST OF FIGURES..... vii

ACKNOWLEDGMENTS..... ix

DEDICATION..... x

CHAPTER 1 INTRODUCTION..... 1

1.1 Historical review..... 1

1.2 Basic equations of electromagnetic induction.. 8

1.3 Voltage..... 17

1.4 Summary of work in this thesis..... 19

CHAPTER 2 FINITE DIFFERENCE EXPRESSIONS FOR VOLTAGE..... 21

2.1 The problem..... 21

2.2 Development of finite difference equations for voltage..... 25

CHAPTER 3 ANALYTIC CONTROL MODEL..... 36

3.1 The model..... 36

3.2 The analytic solution..... 41

3.3 Improved convergence at the boundaries..... 54

3.4 Analytic expressions for voltage..... 60

CHAPTER 4 THE GLOUCESTER FAULT..... 64

4.1 The experiment..... 64

4.2 Transformation of finite difference voltages to fault coordinate system..... 69

4.3 The two-dimensional numerical model..... 75

CHAPTER 5 RESULTS AND DISCUSSION..... 77

5.1 Comparison with analytic model..... 77

5.2 Comparison with Gloucester fault data..... 82

5.3 Conclusion..... 87

REFERENCES..... 89

APPENDIX A PROGRAM LISTINGS..... 93

LIST OF TABLES

Table		Page
5.1.1	Comparison of the true electric field with the analytic and numerical voltage electric field. The voltage fields were assigned to a point midway between the two points which provided the voltage used in each calculation.....	80
5.2.1	Field data: magnitude of 100s sinusoid which maximizes at 21:20:10 in mV/km.....	83
5.2.2	A comparison of electric field amplitudes.....	84

LIST OF FIGURES

Figure		Page
2.1.1	a,b,c. Schematic diagram of the measurement of the voltage between two electrodes grounded in regions with varying conductivity structures.....	22
2.2.1	The general node (m) in the numerical grid for finite difference calculations.....	26
3.1.1	The quarter-space model.....	37
3.1.2	The control model used in this thesis.....	38
4.1.1	Geology and apparent conductivities of the Gloucester fault. Conductivities are from Telford et al. (1977) except for those in brackets which are assumed on the basis of conductivities for similar rock types in the area.....	65
4.1.2	Electric field data from the Gloucester fault, Ontario, Canada.....	66
4.1.3	Orientation and position of the electrode profile in the Gloucester fault area.....	67

Figure		Page
4.2.1	Notation used in the numerical program to transform the electric fields along the electrode profile to fields perpendicular and parallel to the strike.....	71
4.3.1	An idealized model of the Gloucester fault used in the numerical calculations.....	76
5.1.1	A graphical comparison of the real true electric field and the corresponding values obtained from voltage divided by separation distance. Note that analytic and numerical voltage electric field values are so close as to be indistinguishable on the graph.....	78
5.1.2	A graphical comparison of the imaginary true electric field and the corresponding values obtained from voltage divided by separation distance. Note that analytic and numerical voltage electric field values are so close as to be indistinguishable on the graph.....	79

ACKNOWLEDGMENTS

I am greatly indebted to my supervisor, Dr. J.T. Weaver, for his invaluable support and guidance throughout this work.

I also wish to thank Dr. Alan G. Jones for starting it all and Andrew, Todd and Kim for being my "software consultants" during the word-processing of this thesis.

Financial support provided from funds in Dr. Weaver's National Research Council Operating grant A3830 is gratefully acknowledged.

DEDICATION

To my father

(Dad-thanks for the footsteps-Leem)

CHAPTER 1

INTRODUCTION

1.1 Historical Review

Observations at the surface of the Earth of the electromagnetic field due to sources in the ionosphere have long been studied for the information they can provide about the Earth's conductivity structure. Studies have been performed both globally, when the overall conductivity structure at great depth (ie.~1000km) is of interest, and regionally, when the emphasis is on finer details of the crust and upper mantle (ie.~100km). Global studies, reviewed by Rikitake (1973), will not be discussed further as this thesis is concerned only with electromagnetic problems of a local nature in which lateral conductivity inhomogeneities occur.

There are two techniques for determining conductivity in the earth; "inversion" and "forward modelling". The former is dependent on the latter. In the "inversion" technique a conductivity distribution is deduced from observed results which have been fed into an algorithm. Although,

theoretically a unique solution can be derived from exact data for all frequencies, inversion methods involve many mathematical difficulties because all data are band-limited and inaccurate to some extent. The less sophisticated approach is simple "forward modelling" which requires the computation of some observable response, given the primary field and distribution of conductivity. It then compares the calculated response with that observed and if they do not coincide (within some error limit of the data) the model is changed and the procedure repeated. "Forward modelling" is still the technique most often used in determining the conductivity distribution in two and three-dimensional models.

For regional studies the Earth may be considered flat. In a now classic paper by Price (1950), a general treatment of electromagnetic induction problems for such a flat Earth is discussed. Price analyzed the problem of a homogeneous conducting half-space (an approximation for the Earth) acted upon by an arbitrary known source field above it. Weaver (1971) simplified Price's theory by using integral transforms and by the introduction of electric and magnetic Hertz vectors. This has since been generalized to the case of electromagnetic induction in an n-layered conducting half-space the principal features of which have been reviewed by

Weaver (1973).

Lateral variations in conductivity have been studied both analytically and numerically. Because of the mathematical difficulties encountered analytic solutions are only practical for problems of simple geometry. Yet, although analytic solutions are limited to a few simple models, they are extremely useful as accuracy checks on the various numerical techniques in use. The first analytic solution of electromagnetic induction in an earth with lateral conductivity variations was obtained by d'Erceville and Kunetz (1962) who considered the effect of a vertical contact between two homogeneous media with contrasting conductivity. Rankin (1962) extended their solution to treat a vertical dike embedded in a homogeneous structure. In solutions of this type the magnetic vector is polarized parallel to the strike and the basement region is idealized as a perfect electric (or perfect magnetic) conductor. It should be noted that nearly all successful analytic solutions are for the B-polarization problems where the horizontal magnetic field of the source is polarized parallel to the strike. E-polarizations problems, where the horizontal magnetic field of the source is perpendicular to the strike, are much harder to analyse. Weaver (1963) extended the vertical contact to an infinite basement depth. More recently, Geyer (1972)

considered the effect of a dipping contact between two homogeneous regions. Solutions have also been obtained for models with more than one vertical contact (ie. the "segmented overburden" model of Wait and Spies, 1974 - also discussed by Wait, 1982, and the similar model of Weaver, Le Quang and Fischer, 1985). The analytic solution discussed in this thesis, except for a slight change in notation, is that of Weaver, Le Quang and Fischer (1985) and the control model used is identical to the one they employ.

Various numerical techniques have been used to analyse problems involving more complex structures --- finite difference, finite element, integral equation and transmission line analogy for example. A review of some numerical methods is found in the treatment by Ward et al. (1973). Many modelling programs have been developed which employ these techniques (sometimes combined with analytic methods to speed the computation) such as the finite difference program of Brewitt-Taylor and Weaver (1976) and the finite element program of Wannemaker (1987). Finite difference methods are capable of solving very general electromagnetic induction problems but for the more complex of these, large amounts of computer time and computer storage space is required. Analogue models (see review by Dosso, 1973) have proved useful for the study of very complex three-

dimensional conductivity structures which cannot be treated by numerical modelling because of the limitations imposed by the coarseness of the numerical grid.

The study of near-surface lateral inhomogeneities was greatly simplified by Price (1949) who introduced the "thin-sheet" approximation. In this approach the Earth is mathematically represented by an infinitely thin sheet of variable integrated conductivity underlain by a non-conducting medium. Rikitake (1966) took into account the effect of a highly conducting mantle by adding a conducting half-space under the non-conducting region. The "coast-effect" has been extensively studied by incorporation of discontinuities into the integrated conductivity of the thin sheet (see eg. Roden, 1964; Ashour, 1971). An important observation from these studies is that the vertical magnetic field is enhanced at the coastline (or continental shelf) dropping off rapidly seawards and more slowly inland.

In strictly two-dimensional flat Earth models with electrically isolated thin sheets, only the E-polarization mode is of importance for electromagnetic induction. A second type of model has the thin sheet in contact with the underlying layered structure, permitting vertical current flow into and out of the sheet. For strictly two-dimensional problems only the B-polarization mode admits vertical current

loops (ie. the 'poloidal' mode). Weidelt (1971) obtained an analytic E-polarization solution for the case of one plane, situated in free space, consisting of two half-sheets of differing (finite) integrated conductivities and more recently Dawson, Weaver and Raval (1982) and Dawson (1979) have solved the complete problem with a conducting half-space beneath the thin sheet. The corresponding B-polarization problem has been treated analytically by Nicoll and Weaver (1977), Dawson and Weaver (1979), Dawson (1979), and Dawson, Weaver and Raval (1982). Analytic techniques serve as valuable checks on numerical procedures for the modelling of arbitrary distributions of integrated conductivity.

Part of the interest in the study of layered half-spaces lies in the magneto-telluric method of inferring underlying conductivities from surface fields measurements at a point. Since the classic paper of Cagniard (1953), who discussed plane waves incident on a layered conductor, numerous papers have been published on this subject (see eg. the review by Wait (1962) and the bibliography in Keller and Kaufman, 1981). Wait (1954) discussed the case of more general sources by extending this to complex angles of incidence.

In the magneto-telluric method of geophysical prospecting it is customary to represent the Earth's crust as a system of parallel layers that are individually

homogeneous. It has been appreciated for some time that lateral variations of the electric and geometrical characteristics will complicate the interpretation. One of these complications (see eg. Fischer, Le Quang and Müller, 1983) is due to the finite separation of the field electrodes which, in the B-polarization mode, are at times deployed across a fault or other sharp discontinuity in conductivity. Fischer et al. (1983) remark on the fact that in this case the measurement obtained from these electrodes cannot yield an accurate value for the electric field but only some value in between the two extremes.

1.2 Basic Equations of Electromagnetic Induction

Maxwell's equations are a mathematical expression of the properties of time-dependent electromagnetic fields. Let $\underline{E}$ and $\underline{H}$ represent the electric and magnetic field intensities, $\underline{D}$ and $\underline{B}$ the electric and magnetic flux densities and $\underline{J}$ and ρ the volume current and charge densities. All these quantites are dependent on the space variables (x,y,z) and on time t, and are related by Maxwell equations which in SI units, are

$$\text{curl } E + \frac{\partial B}{\partial t} = 0 \ , \qquad (1.2.1.a)$$

$$\text{curl } H - \frac{\partial D}{\partial t} = J \ , \qquad (1.2.1.b)$$

$$\text{div } D = \rho , \qquad (1.2.1.c)$$

$$\text{div } B = 0 \ . \qquad (1.2.1.d)$$

These equations can be simplified so that they depend only on $\underline{E}$ and $\underline{B}$ which we will loosely refer to as the electric

and magnetic fields.

In geophysical induction problems all sources are assumed to lie some distance above the Earth's surface and all regions below this are assumed to be linear and isotropic. In such relationships

$$\underline{D} = \varepsilon\underline{E} \ , \qquad \underline{H} = \underline{B} \ / \mu \ , \qquad \underline{J} = \sigma\underline{E} \qquad (1.2.2)$$

hold true with ε being the permittivity, μ the permeability and σ the conductivity of the medium. We also assume that these regions have a permeability of $\mu \approx \mu_0 = 4\pi \times 10^{-7}$ H/m. This is approximately true for most material except ferromagnetic minerals which have $\mu >> \mu_0$. Large differences in magnitude between μ and μ_0 are, however, uncommon and occur in the Earth only in negligible quantities.

It is also assumed that any sources have a common harmonic time dependence with angular frequency ω so that

$$\underline{E} = \underline{E}\,(x,y,z)\, e^{i\omega t} \ , \qquad \underline{B} = \underline{B}\,(x,y,z)\, e^{i\omega t} \ , \qquad (1.2.3)$$

where it is common to write the (complex) spatial part of

the electric and magnetic fields in component form as $\underline{E} \equiv (U,V,W)$ and $\underline{B} \equiv (X,Y,Z)$.

Using the assumptions represented by equations (1.2.2) and (1.2.3) we can rewrite the Maxwell equations (1.2.1) in the simplified form

$$\text{curl}\,\underline{E} + i\omega\underline{B} = 0 \ , \qquad (1.2.4.a)$$

$$\text{div}\,\underline{E} = \frac{\rho}{\varepsilon} \ , \qquad (1.2.4.b)$$

$$\text{curl}\,\underline{B} - i\omega\varepsilon\mu_0\underline{E} = \mu_0\sigma\,\underline{E} \ , \qquad (1.2.4.c)$$

$$\text{div}\,\underline{B} = 0 \ . \qquad (1.2.4.d)$$

For geomagnetic induction studies the displacement current term $i\omega\varepsilon\mu_0\underline{E}$ in (1.2.4.c) can be shown to be negligible with respect to the other terms in the relevant equation. For this to be true in the Earth it is required that

$$\omega << \frac{\sigma}{\varepsilon} \qquad (1.2.5)$$

Since most materials in the Earth's crust have conductivities ranging from 10^{-6}–10^{4} S/m and $1 \leq \varepsilon/\varepsilon_0 \leq 110$ kHz (Jackson 1975 p.16) the above equation (1.2.5) demands only that $\sigma/\varepsilon < 110$ kHz (ie. that frequency $f << 110$ kHz so $\omega = 2\pi f << 509$ rad/s). To allow the neglect of displacement current in free space where $\sigma = 0$ we must satisfy the further constraint that

$$\omega^2 << \frac{1}{\ell^2 \varepsilon \mu_0} \qquad (1.2.6)$$

(see e.g. Green 1978) where ℓ is the characteristic length in the region under study. For global studies ℓ is of the order of one Earth radius (~6400 km) so that (1.2.6) is valid for $f << 47$ Hz. For this case the upper limit of f is usually said to be 10 Hz. If ℓ is smaller, as it is for local studies, the bound on ω will be correspondingly higher. Since the values of f important in geomagnetic induction studies are generally bounded by $f < 1$ Hz the neglect of displacement currents is justified both in the earth and in free-space regions. Exclusion of the

displacement current term in (1.2.4.c) leaves the simpler form $\text{curl}\,\underline{B} = \mu_0\sigma\underline{E}$.

If it is assumed that the Earth is made up of homogeneous conducting regions we can take the volume charge density to be zero, since any volume charge distribution will quickly decay, independent of any applied field (Jones, 1964, p 12). In air, the volume charge density is also assumed zero so $\rho=0$ everywhere. This fact makes (1.2.4.b), $\text{div}\underline{E}=\rho/\varepsilon$, redundant ($\rho=0$, hence $\text{div}\underline{E}=0$). Using the vector identity $\text{div}\,\text{curl} \equiv 0$ on (1.2.4.c) we are left with $0=\text{div}(\mu_0\sigma\underline{E})$. In the homogeneous regions under consideration μ_0 and σ are both constant so $0=\text{div}\,\underline{E}$ is obtained without the need for equation (1.2.4.b).

Another redundant equation is (1.2.4.d) which can be obtained from (1.2.4.a) and the vector identity $\text{div}\,\text{curl} \equiv 0$. Elimination of these redundancies leaves the two basic equations of electromagnetic induction:

$$\text{curl}\,\underline{E} = -i\omega\underline{B} \qquad (1.2.7)$$

$$\text{curl}\,\underline{B} = \mu_0\sigma\underline{E} \qquad (1.2.8)$$

In many problems it is convenient to introduce the vector potential $\underline{A}$ given by

$$\text{curl}\,\underline{A} = \underline{B}. \tag{1.2.8}$$

So (1.2.1.a) can be written as

$$\text{curl}\,(\underline{E} + \frac{\partial \underline{A}}{\partial t}) = 0. \tag{1.2.9}$$

Thus, for the time-dependent case, we no longer have $\underline{E}=-\text{grad}\phi$ (which is true for static fields where $\text{curl}\underline{E}=0$, and ϕ is the scalar potential), but now it is the quantity in equation (1.2.9) whose curl vanishes. Therefore,

$$\underline{E} = -\frac{\partial \underline{A}}{\partial t} - \text{grad}\,\phi. \tag{1.2.10}$$

Hence the electric field $\underline{E}$ can arise both from accumulation of charge, through the $-\text{grad}\phi$ term, and from changing magnetic fields, through the $-\partial\underline{A}/\partial t$ term.

B-polarization fields can be completely derived from the one field component X, and similarly E-polarization

fields are derived from U. Thus, for a two-dimensional problem, we can simplify the representation of the field without using potentials.

In two dimensional problems where $\underline{E}$ and $\underline{B}$ are independent of one of the coordinates (say x) the induction equations (1.2.7) and (1.2.8) become

$$\frac{\partial W}{\partial y} - \frac{\partial V}{\partial z} = -i\omega X \tag{1.2.11}$$

$$\frac{\partial X}{\partial z} = \mu_0 \sigma V \tag{1.2.12}$$

$$\frac{\partial X}{\partial y} = -\mu_0 \sigma W \tag{1.2.13}$$

and

$$\frac{\partial Z}{\partial y} - \frac{\partial Y}{\partial z} = \mu_0 \sigma U \tag{1.2.14}$$

$$\frac{\partial U}{\partial z} = -i\omega Y \tag{1.2.15}$$

$$\frac{\partial U}{\partial y} = i\omega Z \tag{1.2.16}$$

where we recall that $\underline{B}=(X,Y,Z)$ and $\underline{E}=(U,V,W)$.

It is well known that in the source-free region these equations fall into two independent groups (see e.g. Weaver 1963). The field has decoupled into the B-polarization or transverse magnetic (TM) node associalted with (1.2.11), (1.2.12) and (1.2.13) and the E-polarization or transverse electric (TE) mode associated with (1.1.124), (1.2.15), and (1.2.16). The B-polarization problem involves only the X, Y and W components and the field in this case can be written as

$$\underline{B} = (X,0,0), \qquad \underline{E} = (0,V,W). \tag{1.2.17}$$

Similarly the E-polarization problem involves only the Y, Z and U components and its field is given by

$$\underline{B} = (0,Y,Z), \qquad \underline{E} = (U,0,0). \tag{1.2.18}$$

For any two-dimensional problem thse modes can be treated separately and the overall fields found by linear superposition. For the B-polarization problem it is

obvious from (1.2.12) and (1.2.13) that in a non-conducting region ($\sigma=0$) $\partial X/\partial y=0$ and $\partial X/\partial z=0$ so that

$$X = X_0 \quad \text{(constant)} \tag{1.2.19}$$

1.3 Voltage

The voltage v_{ab} between two points a and b is defined as (see eg. Moon and Spencer,)

$$v_{ab} = \int_a^b \underline{\mathcal{F}} \cdot \underline{ds} \qquad (1.3.1)$$

where $\underline{\mathcal{F}}$ is the force per unit charge given by

$$\underline{\mathcal{F}} = \underline{E} + (\underline{v} \times \underline{B}) \qquad (1.3.2)$$

and $\underline{v}$ is the velocity of a test charge with respect to the coordinate system in which $\underline{E}$ and $\underline{B}$ are given. In the static case $\underline{\mathcal{F}} = \underline{E}$ and $\underline{E}$=-gradϕ (ϕ=scalar potential) so the voltage is simply the difference in potentials at a and b and hence is independent of the path of integration. However, in a general time-dependent case, $\underline{E}$ is given by equation (1.2.10). Using this definition for $\underline{E}$ in (1.3.1) we obtain

$$v_{ab} = -\int_a^b \text{grad}\phi \cdot \underline{ds} - \frac{\partial}{\partial t}\int_a^b \underline{A} \cdot \underline{ds} \,. \qquad (1.3.3)$$

The first integral is simply the potential difference $\phi_b - \phi_a$ so (1.3.3) becomes

$$v_{ab} = \phi_a - \phi_b - \frac{\partial}{\partial t}\int_a^b \underline{A} \cdot \underline{ds} \,. \qquad (1.3.4)$$

As mentioned above, the second integral vanishes in the static case and the voltage is equal to the potential difference. But for most time-dependent fields this is not the case and v_{ab} depends on the path of integration.

1.4 Summary of work in this thesis

In this thesis a method is developed to modify an existing two-dimensional finite difference program so that voltages rather than electric fields are calculated at each node of the numerical grid in the B-polarization model. The numerical results are checked against the exact analytical expressions for voltage obtained for the control model of Weaver, Le Quang and Fischer (1985). Furthermore, a modification of the analytic solution is made to improve its convergence at boundaries between regions of different conductivities. The geology and experimental set up of the Gloucester fault region in Canada is dicussed and notation is introduced to deal with the problem of strikes that are not perpendicular to the electrode line. The equations used to calculate the electric field from the finite difference voltages must be amended according to this new notation.

Finally a two-dimensional model for the area is proposed and real data obtained over the Gloucester fault

are compared with results given by finite difference modelling based on voltages and on the more traditional electric field calculations. The results are then discussed with the aim of pointing out some of the errors inherent in the magnetotelluric studies of such regions.

CHAPTER 2

FINITE DIFFERENCE EXPRESSIONS FOR VOLTAGE

2.1 The problem

In applications of the magnetotelluric method the electric field is measured by recording the voltage between two grounded electrodes and dividing by their separation distance. In the schematic diagram Figure 2.1.1 (a) the electric field in the y-direction would be given by

$$E_y = \frac{v_{21}}{d} \qquad (2.1.1)$$

where v_{21} is the recorded voltage between electrode 2 and electrode 1. The electric field measured in this manner is then arbitrarily assigned to a particular point in the range covered by the electrode pair. Typically it is chosen to be at one of the electrode

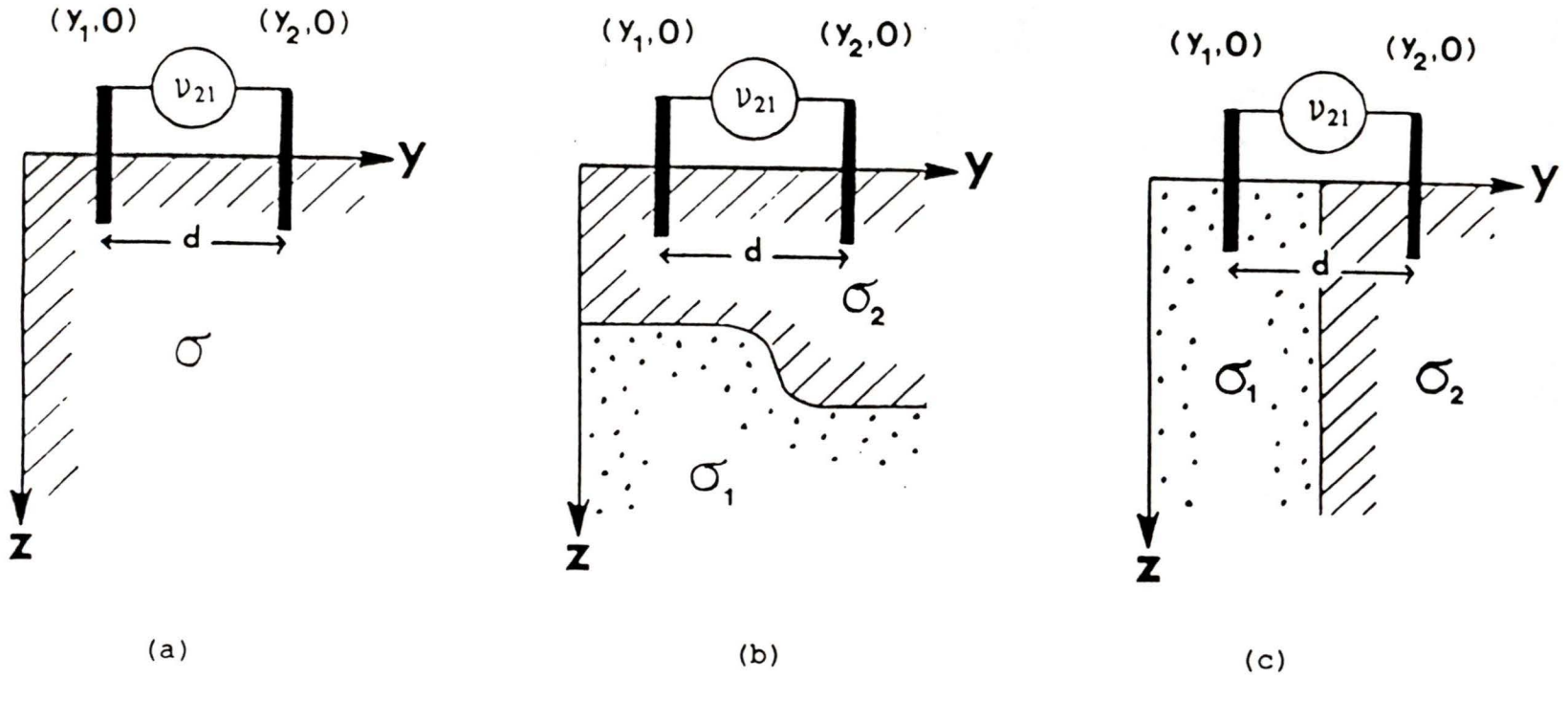

Figure 2.1.1 Schematic diagram of the measurement of the voltage between two electrodes grounded in regions with varying conductivity structure.

positions although the point midway between the electrodes would seem to be preferable.

Actually, from (1.2.25), the voltage between the two electrodes is correctly defined by the line integral

$$v_{21} = \int_1^2 \underline{E} \cdot \underline{ds} = \int_{y_1}^{y_2} E_y \, dy \ , \qquad (2.1.2)$$

which agrees with (2.1.1) only if E_y is constant between the electrodes. Note that in general the line integral (2.1.2) is path dependent, but for the application considered in this thesis the value of v_{21} is always independent of the path of integration. In regions with near-surface inhomogeneities such as shown in Figure 2.1.1 (b), (2.1.1) will give some average value for E_y, while in the extreme case shown in Figure 2.1.1 (c) where the electrodes are embedded in surface materials of different conductivities σ_1 and σ_2, E_y is actually discontinuous across the boundary between the two regions and (2.1.1) is no longer valid. Note that the electric field in these equations is the field given by equation (1.2.20) ($\underline{E}=-\text{grad}\Phi-\partial\underline{A}/\partial t$) where Φ is the scalar potential, gradΦ is the

field due to charge accumulations on conductivity boundaries and $\underline{A}$ is the vector potential. $\partial\underline{A}/\partial t$ is the induced voltage driving the telluric currents. Both terms will be present in the configuration shown in Figure 2.1.1(c).

Thus, in general, electric fields measured by voltages are not the true electric fields given by numerical modelling programs. In order to compare model with experiment on an equal basis it is therefore proposed that voltage divided by electrode separation be used as the "electric field" in model calculations when comparisons with real data are made. For two-dimensional calculations, only the B-polarization formulae will require modification; the electric field in the E-polarization mode, the field determined between electrodes parallel to the strike in the x-direction, will not be affected by variations in y of the conductivity.

Existing two-dimensional finite difference programs can be amended so that voltages between nodes rather than electric fields are calculated at each node of the numerical grid in the B-polarization model.

2.2 Development of finite difference equations for voltage

Since it is ν_{21} rather than E_y that is measured in magnetotelluric sounding it is desirable to calculate the voltage between the grid points on the surface of a two-dimensional numerical model. Consider a node $y=y_m$ $(m=2,3\ldots,M-1)$ as shown in Figure 2.2.1 The notation we use is the same as in Brewitt-Taylor and Weaver (1976) (also Weaver, Le Quang and Fischer, 1985) except that the second subscripts on the parameters (indicating the grid coordinate number in the z-direction) are omitted since we are working on the surface z=0. The y and z components of the electric field are denoted by V(y,z) and W(y,z) respectively and at the surface nodes we write $V(y_m\pm 0,0)=V_m^{\pm}$, $W(y_m\pm 0,0)=W_m$ the latter being uniquely defined by continuity of the tangential electric field.

We also define the apparent resistivities

$$\rho_{m\pm 1/2} = \frac{1}{\omega\mu_0\sigma_{m\pm 1/2}}, \qquad \rho_m = \frac{h_{m-1}\rho_{m-1/2} + h_m\rho_{m+1/2}}{h_{m-1} + h_m}. \quad (2.2.1)$$

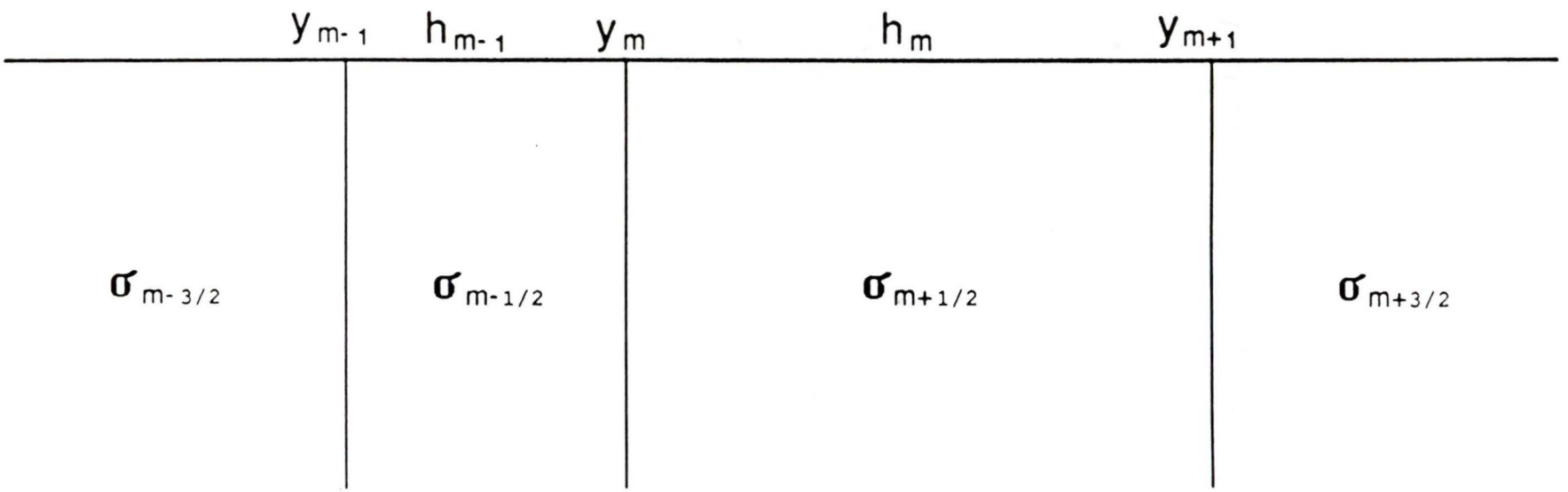

Figure 2.2.1 The general node (m) in the numerical grid for finite difference calculations.

On the boundaries continuity of normal current density j_y requires

$$\frac{V_m^-}{\rho_{m-1/2}} = \frac{V_m^+}{\rho_{m+1/2}} \qquad (=\omega\mu_0 (j_y)_m) \qquad (2.2.2)$$

Since div $\underline{E}$ = 0 in each cell of constant conductivity

$$\frac{\partial V}{\partial y} + \frac{\partial W}{\partial z} = 0 \qquad (2.2.3)$$

and W is continous across $y=y_m$ implying that $\partial W/\partial z$ is also continuous. Hence

$$\left(\frac{\partial V}{\partial y}\right)_m^- = -\left(\frac{\partial W}{\partial z}\right)_m^- = -\left(\frac{\partial W}{\partial z}\right)_m^+ = \left(\frac{\partial V}{\partial y}\right)_m^+ . \qquad (2.2.4)$$

Since $\underline{E}$ satisfies $\nabla^2\underline{E}=i\omega\mu_0\sigma\underline{E}$ in each cell of uniform conductivity σ we have

$$\left(\frac{\partial^2 V}{\partial y^2}\right)_m^+ = i\,\frac{V_m^+}{\rho_{m+1/2}} - \left(\frac{\partial^2 V}{\partial z^2}\right)_m^+ . \qquad (2.2.5)$$

By using (2.2.2) as a substitution in both terms on the right hand side we obtain

$$\left(\frac{\partial^2 V}{\partial y^2}\right)_m^+ = i\,\frac{V_m^-}{\rho_{m-1/2}} - \rho_{m+1/2}\,\frac{\partial^2}{\partial z^2}\left(\frac{V_m^-}{\rho_{m-1/2}}\right). \qquad (2.2.6)$$

Using the V_m^- version of equation (2.2.5)

$$\frac{\partial^2}{\partial z^2}\,(V_m^-) = i\,\frac{V_m^-}{\rho_{m-1/2}} - \left(\frac{\partial^2 V}{\partial y^2}\right)_m^- \qquad (2.2.7)$$

we can solve for $\frac{\partial^2}{\partial z^2}\left(\frac{V_m^-}{\rho_{m-1/2}}\right)$ which can then be used in (2.2.6) to give

$$\left(\frac{\partial^2 V}{\partial y^2}\right)_m^+ = i\,\frac{V_m^-}{\rho_{m-1/2}} - i\,\frac{\rho_{m+1/2}}{\rho_{m-1/2}^2}\,V_m^- + \frac{\rho_{m+1/2}}{\rho_{m-1/2}}\left(\frac{\partial^2 V}{\partial y^2}\right)_m^- \qquad (2.2.8)$$

The results (2.2.2), (2.2.4) and (2.2.8) constitute boundary conditions on the (discontinuous) fields V and $\partial^2 V/\partial y^2$ at a surface node on the vertical boundary between two cells of different conductivity. Boundary condition (2.2.4) shows

that $\partial V/\partial y$ is continuous at such a node.

The finite difference program of Brewitt-Taylor and Weaver (1976) is based on central difference formulae which are obtained by expanding the field up to second order terms, and it is therefore necessary to calculate voltages to the same accuracy. A Taylor expansion of V on either side of the node y_m yields

$$V_{m+1}^{-} = V_m^{+} + h_m \left(\frac{\partial V}{\partial y}\right)_m^{+} + \frac{h_m^2}{2} \left(\frac{\partial^2 V}{\partial y^2}\right)_m^{+} , \qquad (2.2.9)$$

$$V_{m-1}^{-} = V_m^{-} - h_{m-1} \left(\frac{\partial V}{\partial y}\right)_m^{-} + \frac{h_{m-1}^2}{2} \left(\frac{\partial^2 V}{\partial y^2}\right)_m^{-} . \qquad (2.2.10)$$

Adding (2.2.9) multiplied by h_{m-1} to (2.2.10) multiplied by h_m and using boundary condition (2.2.4), $\left(\frac{\partial V}{\partial y}\right)_m^{+} = \left(\frac{\partial V}{\partial y}\right)_m^{-}$, we obtain

$$h_{m-1}V_{m+1}^{-} + h_m V_{m-1}^{+} = h_{m-1}V_m^{+} + h_m V_m^{-} + \frac{1}{2} h_m h_{m-1}\left[h_m \left(\frac{\partial^2 V}{\partial y^2}\right)_m^{+} + h_{m-1}\left(\frac{\partial^2 V}{\partial y^2}\right)_m^{-}\right]. \qquad (2.2.11)$$

Substituting boundary condition (2.2.8) and using the definition of ρ_m given in (2.2.1) we obtain

$$\frac{1}{2} h_m h_{m-1} \left(\frac{\partial^2 V}{\partial y^2}\right)_m^+ \frac{h_m+h_{m-1}}{\rho_{m-1}} \rho_m - \frac{1}{2} h_m h_{m-1}^2 \left(\frac{1}{\rho_{m+1/2}} - \frac{1}{\rho_{m-1/2}}\right) V_m^-$$

$$= h_{m-1} (V_{m+1}^- - V_m^+) + h_m (V_{m-1}^+ - V_m^-) \qquad (2.2.12)$$

Rearrangment of this results in

$$\left(\frac{\partial^2 V}{\partial y^2}\right)_m^+ = \frac{2\rho_{m+1/2}}{\rho_m (h_m+h_{m-1})} \left\{\frac{V_{m+1}^- - V_m^+}{h_m} - \frac{V_m^- - V_{m-1}^+}{h_{m-1}}\right\}$$

$$+ \frac{i h_{m-1} V_m^-}{\rho_m (h_m+h_{m-1})} \left(1 - \frac{\rho_{m+1/2}}{\rho_{m-1/2}}\right) \qquad (2.2.13)$$

This is a generalization of the finite difference formula for $\partial^2 V/\partial y^2$ at a conductivity boundary. If $\rho_{m+1/2}=\rho_{m-1/2}=\rho_m$ it reduces to the familiar central difference representation of the second derivative. To find an expression for the voltage between the nodes y_m and y_{m+1} we represent V in $y_m<y<y_{m+1}$ by the Taylor expansion

$$V(y) = V_m^+ + (y-y_m)\left(\frac{\partial V}{\partial y}\right)_m^+ + \frac{(y-y_m)^2}{2}\left(\frac{\partial^2 V}{\partial y^2}\right)_m^+ \qquad (2.2.14)$$

Now we integrate this equation according to (2.1.2)

$$\nu_{m+1,m} = V_m^+ \int_0^{h_m} du + \left(\frac{\partial V}{\partial y}\right)_m^+ \int_0^{h_m} u\,du + \frac{1}{2}\left(\frac{\partial^2 V}{\partial y^2}\right)_m^+ \int_0^{h_m} u^2\,du \qquad (2.2.15)$$

$$= h_m V_m^+ + \frac{1}{2} h_m^2 \left(\frac{\partial V}{\partial y}\right)_m^+ + \frac{1}{6} h_m^3 \left(\frac{\partial^2 V}{\partial y^2}\right)_m^+ \qquad (2.2.16)$$

Using (2.2.9) to eliminate $\left(\frac{\partial V}{\partial y}\right)_m^+$ from the above equation we find that

$$\nu_{m+1,m} = \frac{1}{2} h_m (V_m^+ + V_{m+1}^-) - \frac{h_m^3}{12}\left(\frac{\partial^2 V}{\partial y^2}\right)_m^+ \qquad (2.2.17)$$

where $\left(\frac{\partial^2 V}{\partial y^2}\right)_m^+$ is given by (2.2.12). To avoid two separate calculations of the electric field (one for the right hand

side values V_m^+ and one for the left hand side values V_m^-) everything can be expressed in terms of right hand side values through boundary condition (2.2.2). Thus (2.2.13) becomes

$$\left(\frac{\partial^2 V}{\partial y^2}\right)_m^+ = \frac{2\rho_{m+1/2}}{\rho_m(h_m+h_{m-1})}\left\{\frac{\rho_{m+1/2}V_{m+1}^+}{h_m\rho_{m+3/2}} + \frac{V_{m-1}^+}{h_{m-1}} - V_m^+\left(\frac{1}{h_m} + \frac{\rho_{m-1/2}}{h_{m-1}\rho_{m+1/2}}\right.\right.$$

$$\left.\left. + \frac{ih_{m-1}}{2\rho_{m+1/2}}\left[1 - \frac{\rho_{m-1/2}}{\rho_{m+1/2}}\right]\right)\right\} \qquad (2.2.18)$$

and this is substituted in the equation below which follows from (2.2.17)

$$\nu_{m+1,m} = \frac{1}{2}h_m\left(V_m^+ + \frac{\rho_{m+1/2}}{\rho_{m+3/2}}V_{m+1}^-\right) - \frac{h_m^3}{12}\left(\frac{\partial^2 V}{\partial y^2}\right)_m^+ \qquad (2.2.19)$$

$$= h_m\frac{\rho_{m+1/2}}{2\rho_{m+3/2}}V_{m+1}^-\left\{1 - \frac{\rho_{m+1/2}h_m}{3\rho_m(h_m+h_{m-1})}\right\} - \frac{\rho_{m+1/2}h_m^3V_{m-1}^+}{6\rho_m h_{m-1}(h_m+h_{m-1})}$$

$$+ V_m^+\frac{h_m}{2}\left\{1 + \frac{\rho_{m+1/2}h_m^2}{3\rho_m(h_m+h_{m-1})}\left[\frac{1}{h_m} + \frac{\rho_{m-1/2}}{\rho_{m+1/2}h_{m-1}} + \frac{ih_{m-1}}{2\rho_{m+1/2}}\left(1 - \frac{\rho_{m-1/2}}{\rho_{m+1/2}}\right)\right]\right.$$

Rearrangment of this yields the result

$$\nu_{m+1,m} = \frac{h_m V_m^+}{6\rho_m (h_m+h_{m-1})} \left[h_m\rho_{m+1/2} + 3h_{m-1}\rho_{m-1/2} + 3h_m\rho_{m+1/2} + \frac{h_m^2}{h_{m-1}}\rho_{m-1/} \right.$$

$$\left. + i\,\frac{h_{m-1}h_m^2}{2}\left(1-\frac{\rho_{m-1/2}}{\rho_{m+1/2}}\right)\right]$$

$$- \frac{h_m\rho_{m+1/2}V_{m+1}^+}{6\rho_m\rho_{m+3/2}(h_m+h_{m-1})}\left[-3h_m\rho_{m+1/2} - 3h_{m-1}\rho_{m-1/2} + h_m\rho_{m+1/2} \right]$$

$$- \frac{h_m^3\rho_{m+1/2}V_{m-1}^+}{6\rho_m h_{m-1}(h_m+h_{m-1})}$$

or, on further simplification,

$$\nu_{m+1,m} = \frac{h_m^2}{6\rho_m (h_m+h_{m-1})} \left[\left\{ 4\rho_{m+1/2} + \frac{3h_{m-1}^2 + h_m^2}{h_m h_{m-1}}\rho_{m-1/2} \right.\right.$$

$$\left.\left. + i\,\frac{h_{m-1}h_m}{2}\left(1-\frac{\rho_{m-1/2}}{\rho_{m+1/2}}\right)\right\} V_m^+ \right.$$

$$\left. + \left\{ 2\rho_{m+1/2} + 3\,\frac{h_{m-1}}{h_m}\rho_{m-1/2} \right\} \frac{\rho_{m+1/2}}{\rho_{m+3/2}} V_{m+1}^+ - \frac{h_m}{h_{m-1}}\rho_{m+1/2}\, V_{m-1}^+ \right]$$

which finally reduces to

$$v_{m+1,m} = \frac{h_m^2 \rho_{m+1/2}}{6\rho_m (h_m + h_{m-1})} \left[\left\{ 4 + \left(3\frac{h_{m-1}}{h_m} + \frac{h_m}{h_{m-1}} \right) \frac{\rho_{m-1/2}}{\rho_{m+1/2}} + i \frac{h_{m-1} h_m}{2\rho_{m+1/2}} \left(1 - \frac{\rho_{m-1/2}}{\rho_{m+1/2}} \right) \right\} V_{\bar{m}} \right.$$

$$\left. + \left\{ 2 \frac{\rho_{m+1/2}}{\rho_{m+3/2}} + 3 \frac{h_{m-1}}{h_m} \frac{\rho_{m+1/2}}{\rho_{m+3/2}} \right\} V_{m+1}^{+} - \frac{h_m}{h_{m-1}} V_{m-1}^{+} \right] \qquad (2.2.$$

(m=2,...,M-1), which is the desired finite difference formula giving the voltage between two adjacent nodes on the surface of the numerical grid.

If required, a similar expression can be derived in terms of the left hand side values $V_{\bar{m}}$

$$v_{m+1,m} = \frac{h_m^2 \rho_{m+1/2}}{6\rho_m (h_m + h_{m-1})} \left[\left\{ 4 \frac{\rho_{m+1/2}}{\rho_{m-1/2}} + \left(3\frac{h_{m-1}}{h_m} + \frac{h_m}{h_{m-1}} \right) + i \frac{h_{m-1} h_m}{2\rho_{m+1/2}} \left(\frac{\rho_{m+1/2}}{\rho_{m-1/2}} - 1 \right) \right\} V \right.$$

$$\left. + \left\{ 2 + 3 \frac{h_{m-1}}{h_m} \frac{\rho_{m-1/2}}{\rho_{m+1/2}} \right\} V_{m+1}^{-} - \frac{h_m}{h_{m-1}} \frac{\rho_{m-1/2}}{\rho_{m-3/2}} V_{m-1}^{+} \right] \qquad (2.2.$$

It is worth noting that if the near surface inhomogeneities

do not actually reach the surface itself (as in Figure 2.1.1 (b) for example), so that $\rho_{m-1/2}=\rho_{m+1/2}=\rho_{m+3/2}=\rho_m$, then (2.2.20) and (2.2.21) both reduce to the simplified form

$$\nu_{m+1,m} = \frac{h_m^2}{6(h_m+h_{m-1})}\left[\left\{4 + \left(3\frac{h_{m-1}}{h_m} + \frac{h_m}{h_{m-1}}\right)\right\} V_m \right.$$

$$\left. + \left\{2+3\frac{h_{m-1}}{h_m}\right\} V_{m+1} - \frac{h_m}{h_{m-1}} V_{m-1}\right]. \qquad (2.2.21)$$

If we define $r_m=h_m/h_{m-1}$ and $s_m=r_m/(1+r_m)$ this can be written as

$$\nu_{m+1,m} = \frac{h_m}{6}\left[(3+r_m)V_m - r_m s_m V_{m-1} + (3-s_m)V_{m+1}\right] \qquad (2.2.23)$$

In this case there is, of course, no longer any difference between V_m^+ and V_m^-.

CHAPTER 3

ANALYTIC CONTROL MODEL

3.1 The model

In order to check the accuracy of the equations obtained in the previous chapter it is desirable to have a computer program for calculating these values analytically. The model used in such a program is limited only to those with the simplest of structures because the difficulty of obtaining an analytic solution for a model increases enormously with the increase in complexity of its structure. One of the most simple of these models which has been used of late is the quarter-space model shown in Figure 3.1.1. This model and its analytic solution by d'Erceville and Kunetz (1962) and Weaver (1963) have been used in comparisons with the numerical results of many finite difference programs. A more general control model is one in which there are not two but three different conductive segments overlying a perfect conductor as shown in Figure 3.1.2.

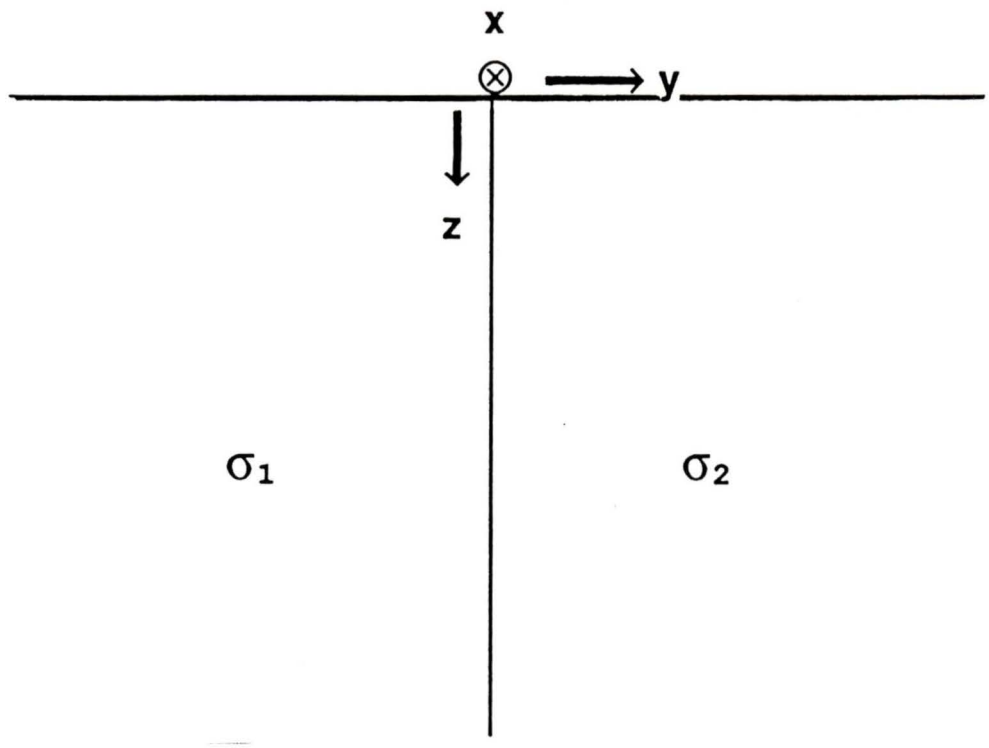

Figure 3.1.1 The quarter-space model

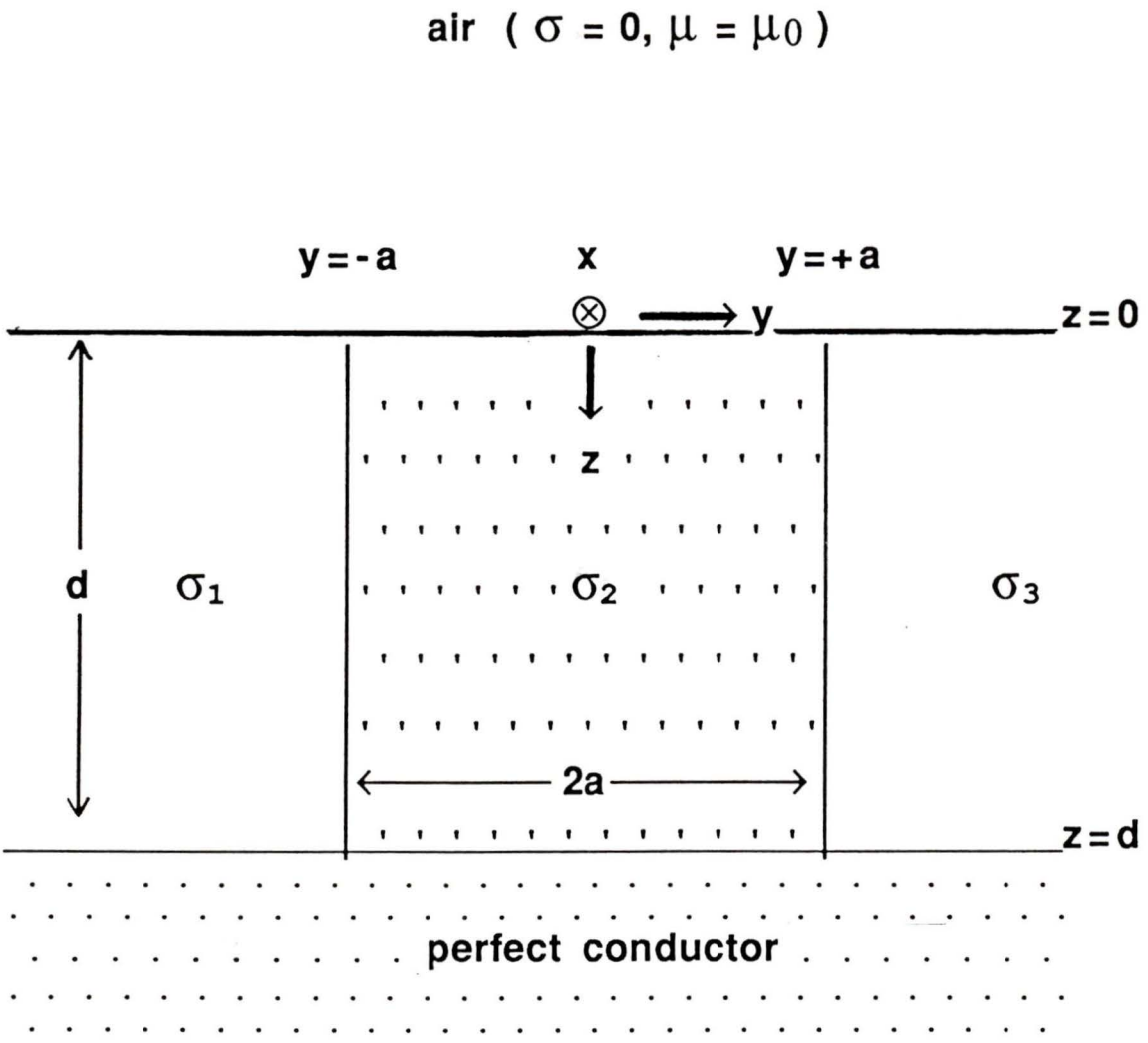

Figure 3.1.2 The control model used in this thesis

This model, being more complex, is a better check on numerical programs. It is similar to the "segmented overburden" model of Wait and Spies (1974) except that they used a perfect insulator for the basement instead of a perfect conductor.

In a rectangular coordinates (x,y,z) it is composed of a conducting plate of thickness d in the region $0<z<d$ with an underlying perfect conductor at $z=d$. The plate is divided into three region $y<-a$, $|y|<a$, and $y>a$, of conductivities σ_1, σ_2, and σ_3 respectively. In the half space $z<0$ we assume a perfect insulator and vacuum permeability μ_0.

There are many advantages to using the model described above. This model can easily simulate such geological structures as the dike ($\sigma_1=\sigma_3$), the vertical fault ($\sigma_2=\sigma_3$), the quarter space model ($\sigma_2=\sigma_3$, $d\rightarrow\infty$), and transition zones where the conductivity changes gradually over three successive cells ($\sigma_1<\sigma_2<\sigma_3$). For this last application small conductivity contrasts are required and 2a should be chosen small so that it equals the node separation in the numerical grid. Another advantage of the three cell model

is that the effect of both high and low conductivity contrasts can be examined simultaneously by choosing (say) $\sigma_2/\sigma_1>10$, $1<\sigma_2/\sigma_3<5$. It is also useful for testing programs which can only handle 'anomalous' regions of finite horizontal extent embedded in a 'normal' one-dimensional structure ($\sigma_1=\sigma_3$) and the perfect conductor at depth d limits the size of the numerical grid (thereby saving CPU time) and provides a clean cut-off to the model.

3.2 The analytic solution

In the now classic paper of d'Erceville and Kunetz (1962) the effect of a vertical contact between two homogeneous media with contrasting geometry was considered. Rankin (1962) used the same method to treat a vertical dike. Wait and Spies (1974) extended these solutions to solve the problem of the segmented overburden model with a perfect insulator basement (see Figure 3.2.2). A similar solution was obtained by Weaver, Le Quang and Fischer (1985) for the perfect conductor version. This solution will be developed here along with the resulting analytic expressions for voltage obtained from the equations for the electric field components.

In the half space $z<0$ we assume a perfect insulator and vacuum permeability μ_0. The field vectors are assumed to depend only on y and z and to have a time dependence $\exp(i\omega t)$ where ω is small enough that displacement currents can be neglected. Then for the B-polarization field under examination the spatial parts of the electric

and magnetic fields can be written in the component form

$$\underline{E}(y,z)=(0,V,W), \qquad \underline{B}(y,z)=(X,0,0). \qquad (3.2.1)$$

In a region of conductivity σ substitution of these components into the equations of electromagnetic induction, (1.2.7) and (1.2.8) gives

$$\frac{\partial X}{\partial z} = \mu_0\sigma V, \qquad \frac{\partial X}{\partial y} = -\mu_0\sigma W, \qquad i\omega X = \frac{\partial V}{\partial z} - \frac{\partial W}{\partial y}, \qquad (3.2.2)$$

which can be used to show that the two dimensional diffusion equation in X, $\nabla^2 X=\alpha^2\partial X/\partial t$ where $\nabla^2 X=\partial^2 X/\partial y^2+\partial^2 X/\partial z^2$, may be written as

$$\frac{\partial^2 X}{\partial y^2} + \frac{\partial^2 X}{\partial z^2} = \mu_0\sigma(i\omega X) + \frac{1}{\sigma}\frac{\partial \sigma}{\partial y}\frac{\partial X}{\partial y} + \frac{1}{\sigma}\frac{\partial \sigma}{\partial z}\frac{\partial X}{\partial z}. \qquad (3.2.3)$$

In regions of constant conductivity σ (3.2.3) becomes

$$\frac{\partial^2 X}{\partial y^2} + \frac{\partial^2 X}{\partial z^2} = i\alpha^2 X \ , \qquad (3.2.4)$$

where $\alpha^2=\omega\mu_0\sigma$. The subscript j (j=1,2,3) is used to differentiate between the values of α, σ and the field components in the three different segments.

In $z<0$ the conductivity is zero. So from (3.2.2) $\partial X/\partial z=0$ and $\partial X/\partial y=0$ indicating that in this region $X=B_0$ (a constant). So we must solve (3.2.4) with $X=X_j$ and $\alpha=\alpha_j$ (j=1,2,3) for $0<z<\infty$ subject to the boundary conditions

i) $X_j=B_0$ on $z=0$;

ii) $\frac{\partial X_j}{\partial z}=0$ on $z=d$;

iii) $X_1=X_2$ and $\sigma_2\frac{\partial X_1}{\partial y} = \sigma_1\frac{\partial X_2}{\partial y}$ on $y=-a$;

iv) $X_2=X_3$ and $\sigma_3\frac{\partial X_2}{\partial y} = \sigma_2\frac{\partial X_3}{\partial y}$ on $y=+a$.

Condition ii) follows from the vanishing of the tangential electric field at the surface of a perfect conductor and iii) and iv) are a consequence of the

continuity of the tangential electric and magnetic fields at a boundary.

At an infinite distance from the boundaries at $y=\pm a$, X is undisturbed by the other conductive regions (ie. $\partial X/\partial y \to 0$ as $|y| \to \infty$) and is independent of y so that (3.2.4) reduces to $\partial^2 X/\partial z^2 = i\alpha^2 X$ which has the general solution

$$\tilde{X}_j = A_j e^{z\alpha_j\sqrt{i}} + B_j e^{-z\alpha_j\sqrt{i}} , \qquad (3.2.5)$$

where the tilda denotes the general solution of the undisturbed field. Since this $\partial\tilde{X}_j/\partial z$ must vanish as $z \to d$ and $\tilde{X}_j = B_0$ at $z=0$ we have the two equations

$$A_j + B_j = B_0 , \qquad A_j e^{d\alpha_j\sqrt{i}} - B_j e^{-d\alpha_j\sqrt{i}} = 0. \qquad (3.2.6)$$

From (3.2.6) it is possible to solve for A_j and B_j

$$A_j = \frac{B_0 e^{-d\alpha_j\sqrt{i}}}{2\cosh(d\alpha_j\sqrt{i})} , \qquad (3.2.7)$$

$$B_j = \frac{B_0 e^{d\alpha_j\sqrt{i}}}{2\cosh(d\alpha_j\sqrt{i})} , \qquad (3.2.8)$$

and hence

$$\tilde{X}_j = B_0 \frac{\cosh[(d-z)\alpha_j\sqrt{i}]}{\cosh(d\alpha_j\sqrt{i})} . \qquad (3.2.9)$$

In each medium fields due to the boundaries are superimposed on these undisturbed fields. If $f_j(y,z)$ represent these disturbances then the total two-dimensional fields are

$$X_j(y,z) = \tilde{X}_j(z) + f_j(y,z) \qquad (3.2.10)$$

where $f_j(y,z)$ satisfies the same differential equation (3.2.4) implying that

$$f_j(y,0) = 0 \quad \text{and} \quad f_j'(y,d) = 0 \qquad (3.2.11)$$

From the boundary conditions iii) and iv) we have the following

$$\tilde{X}_1(z)+f_1(-a,z)=\tilde{X}_2(z)+f_2(-a,z) \ , \tag{3.2.12}$$

$$\tilde{X}_2(z)+f_2(a,z)=\tilde{X}_3(z)+f_3(a,z) \ , \tag{3.2.13}$$

$$\sigma_2\frac{\partial f_1}{\partial y}\Big)_{y=-a} = \sigma_1\frac{\partial f_2}{\partial y}\Big)_{y=-a} \ , \tag{3.2.14}$$

$$\sigma_3\frac{\partial f_2}{\partial y}\Big)_{y=a} = \sigma_2\frac{\partial f_3}{\partial y}\Big)_{y=a} \ , \tag{3.2.15}$$

which can be solved for f_i by separation of the variables. Let $f_j(y,z)=g_j(y)h_j(z)$ so that (3.2.4) becomes

$$\frac{g_j''(y)}{g_j(y)} + \frac{h_j(z)''}{h_j(z)} = i\omega\mu_0\sigma_j \tag{3.2.16}$$

where the prime denotes a derivative with respect to the

dependent variable. If we define a separation constant k^2 (3.2.16) can be decoupled into

$$i\omega\mu_0\sigma_j - \frac{g_j''(y)}{g_j(y)} = -k^2 \quad , \tag{3.2.17}$$

$$\frac{h_j(z)''}{h_j(z)} = -k^2 \quad , \tag{3.2.18}$$

and the solutions will be of the form

$$h_j(z) \sim \sin kz, \ \cos kz \ , \tag{3.2.19}$$

$$g_j(y) \sim e^{y\sqrt{k^2+i\omega\mu_0\sigma_j}} , \qquad e^{-y\sqrt{k^2+i\omega\mu_0\sigma_j}} . \tag{3.2.20}$$

The conditions (3.2.11) require $h_j(z)$ to be of the form $\sin k_m z$ where

$$k_m = \frac{(2m+1)\pi}{2d} \quad . \tag{3.2.21}$$

If we now define $\gamma_m^{(j)}=\sqrt{k_m^2+i\alpha_j^2}$ the general solution in S_2 (the j=2 segment) is of the form

$$f_2(y,z) = \sum_{m=0}^{\infty} \left\{ P_m e^{y\gamma_m^{(2)}} + Q_m e^{-y\gamma_m^{(2)}} \right\} \sin k_m z \ , \qquad (3.2.22)$$

which together with boundary conditions iii) and iv) determines the solutions in S_1 and S_3

$$f_1(y,z) = \frac{\sigma_1}{\sigma_2} \sum_{m=0}^{\infty} \frac{\gamma_m^{(2)}}{\gamma_m^{(1)}} \left\{ P_m e^{-a\gamma_m^{(2)}} - Q_m e^{a\gamma_m^{(2)}} \right\} e^{\gamma_m^{(1)}(y+a)} \sin k_m z \ , \qquad (3.2.23)$$

$$f_3(y,z) = \frac{\sigma_3}{\sigma_2} \sum_{m=0}^{\infty} \frac{\gamma_m^{(2)}}{\gamma_m^{(3)}} \left\{ Q_m e^{-a\gamma_m^{(2)}} - P_m e^{a\gamma_m^{(2)}} \right\} e^{\gamma_m^{(3)}(y-a)} \sin k_m z \ . \qquad (3.2.24)$$

where P_m and Q_m are parameters to be determined later. Note that f_1 and f_3 are both bounded as $y\to-\infty$ and $y\to+\infty$ respectively. The f_j (j=1,2,3) solutions are Fourier

series expansions in z. The key to solving for Q_m and P_m lies in finding $\tilde{X}_j-\tilde{X}_2$ as a Fourier sine series $F_j(z)$. Since

$$\tilde{X}_j-\tilde{X}_2 = B_0 \left\{ \frac{\cosh[(d-z)\alpha_j\sqrt{i}]}{\cosh(d\alpha_j\sqrt{i})} - \frac{\cosh[(d-z)\alpha_2\sqrt{i}]}{\cosh(d\alpha_2\sqrt{i})} \right\},$$

we can find its Fourier sine series

$$F_j(z) = B_0 \sum_{m=0}^{\infty} K_m^{(j)} \sin k_m z , \qquad (3.2.25)$$

for j=1,3 where

$$K_m^{(j)} = \frac{2ik_m(\alpha_2^2-\alpha_j^2)}{d(\gamma_m^{(2)}\gamma_m^{(j)})^2} \qquad (3.2.26)$$

are the Fourier coefficients. Combining (3.2.25) (j=1,3) with (3.2.12) and (3.2.13) results in two equations with two unknowns (P_m and Q_m) which can be solved and

substituted back into the equations for f_j (3.2.22), (3,2.23) and (3.2.24). Then from (3.2.10) and after some algebraic rearrangement the solution can be put into the form

$$\frac{X_j}{B_0} = \frac{\cosh[(d-z)\alpha_j\sqrt{i}]}{\cosh(d\alpha_j\sqrt{i})} + \sum_{m=0}^{\infty} F_m^{(j)} \sin k_m z \qquad (3.2.27)$$

where the Fourier series coefficients are given as

$$F_m^{(j)}(y) = P_m^{(j)} \exp[(a-|y|)\gamma_m^{(j)}], \quad (j=1,3), \qquad (3.2.28)$$

$$F_m^{(2)}(y) = L_m^{(1)} \exp[-(y+a)\gamma_m^{(2)}] + L_m^{(3)} \exp[(y-a)\gamma_m^{(2)}]. \qquad (3.2.29)$$

Here we have defined for j=1,3

$$P_m^{(j)} = \frac{\beta_m^{(j)}}{D_m}\left[2\bar{K}_m^{(j)} \exp(-2a\gamma_m^{(2)}) - K_m^{(j)}\{1+\bar{\beta}_m^{(j)} + (1-\bar{\beta}_m^{(j)}) \exp(-4a\gamma_m^{(2)})\}\right] \qquad (3.2.30)$$

$$L_m^{(j)} = \frac{1}{D_m}\left[(1+\bar{\beta}_m^{(j)})\,K_m^{(j)} - (1-\beta_m^{(j)})\,\bar{K}_m^{(j)}\exp(-2a\gamma_m^{(2)})\right] \qquad (3.2.31)$$

where

$$\bar{K}_m^{(j)} = \frac{K_m^{(j)}\,K_m^{(3)}}{K_m^{(j)}} \quad , \qquad (3.2.32)$$

$$\beta_m^{(j)} = \frac{\gamma_m^{(2)}\,\sigma_j}{\gamma_m^{(j)}\,\sigma_2} \quad , \qquad \bar{\beta}_m^{(j)} = \frac{\beta_m^{(1)}\,\beta_m^{(3)}}{\beta_m^{(j)}} \quad , \qquad (3.2.33)$$

and

$$D_m = (1+\beta_m^{(1)})\,(1+\beta_m^{(3)}) - (1-\beta_m^{(1)})\,(1-\beta_m^{(3)})\exp(-4a\gamma_m^{(2)}) \quad . \qquad (3.2.34)$$

Note that the expression for $F_m^{(2)}(y)$ is quoted here in a slightly different (but equivalent) form from that given by Weaver et al. (1985). This was the formula actually used

in the program, and it is not only algebraically simpler than the one quoted in the previous paper but also more convenient for programming. The electric field components are obtained from (3.2.27) by differentiation according to the induction equations (3.2.2). Thus we have

$$\frac{V_j}{B_0} = \frac{-\omega}{\alpha_j}\left[\frac{\sqrt{i}\sinh[(d-z)\alpha_j\sqrt{i}]}{\cosh(d\alpha_j\sqrt{i})} - \frac{1}{\alpha_j}\sum_{m=0}^{\infty} k_m F_m^{(j)}(y)\cos k_m z\right] \quad (3.2.35)$$

$$\frac{W_j}{B_0} = \frac{-\omega}{\alpha_2^2}\sum_{m=0}^{\infty} \gamma_m^{(2)} G_m^{(j)}(y)\sin k_m z \quad (3.2.36)$$

where

$$G_m^{(j)}(y) = \beta_m^{(j)} P_m^{(j)} \exp[(a-|y|)\gamma_m^{(j)}], \quad (j=1,3), \quad (3.2.37)$$

$$G_m^{(2)}(y) = L_m^{(3)} \exp[(y-a)\gamma_m^{(2)}] - L_m^{(1)} \exp[-(y+a)\gamma_m^{(2)}]. \quad (3.2.38)$$

Except for the change in notation mentioned previously these are the analytical solutions as found by Weaver et al (1985).

3.3 Improved convergence at the boundaries

The Fourier series in (3.2.35) does not converge very quickly at the boundaries y=±a. Since this equation is incorporated into the analytic expression for voltage it is desirable to improve the convergence at these points.

At y=-a-0 the Fourier series from (3.2.35) is

$$S(-a,z) = \sum_{m=0}^{\infty} k_m F_m^{(1)}(-a) \cos k_m z \quad . \tag{3.3.1}$$

The term $k_m F_m^{(1)}$ can be written as

$$k_m F_m^{(1)} = \frac{k_m \gamma_m^{(2)} \sigma_1}{D_m \gamma_m^{(1)} \sigma_2} \left[-K_m^{(1)} (1+\beta_m^{(3)}) + \mathcal{O}(e^{-2a\gamma_m^{(2)}}) \right]$$

$$= - \frac{2i\sigma_1}{\sigma_2 d} (\alpha_2^2 - \alpha_1^2) \frac{k_m^2}{\gamma_m^{(1)3} \gamma_m^{(2)}} \tag{3.3.2}$$

$$\frac{1+\ \sigma_3\gamma_m^{(2)}/\sigma_3\gamma_m^{(2)}}{(1+\beta_m^{(1)})\,(1+\beta_m^{(3)})-(1-\beta_m^{(1)})\,(1-\beta_m^{(3)})\,e^{-4a\gamma_m^{(2)}}}+\mathcal{O}(e^{-2a\gamma_m^{(2)}})$$

where we have made successive substitutions from (3.2.28), (3.2.30), (3.2.32), (3.2.33) and (3.2.34). As $m\to\infty$ $\gamma_m^{(j)}\sim k_m$ and $k_m F_m^{(1)}(-a)$ can be approximated by

$$k_m F_m^{(1)}(-a)\sim \frac{2i\omega\mu_0\sigma_1}{\sigma_2 d}\,\frac{(\sigma_1-\sigma_2)}{k_m^2}\,\frac{1+\ \sigma_3/\sigma_2}{\left(1+\frac{\sigma_1}{\sigma_2}\right)\left(1+\frac{\sigma_3}{\sigma_2}\right)}$$

$$\sim \frac{2i\omega\mu_0\sigma_1}{d}\ \ \frac{\sigma_1-\sigma_2}{\sigma_1+\sigma_2}\ \frac{1}{k_m^2} \qquad (3.3.3)$$

By addition and subtraction of the right hand side of (3.3.3) equation (3.3.1) can be written as

$$S(-a,z)\ =\ \frac{2i\alpha_1^2}{d}\ \ \frac{\sigma_1-\sigma_2}{\sigma_1+\sigma_2}\sum_{m=0}^{\infty}\frac{\cos k_m z}{k_m^2}$$

$$+\sum_{m=0}^{\infty}\left\{k_m F_m(-a)-\frac{2i\alpha_1^2(\sigma_1-\sigma_2)}{dk_m^2(\sigma_1+\sigma_2)}\right\}\cos k_m z \quad . \qquad (3.3.4)$$

Now

$$\sum_{m=0}^{\infty}\frac{\cos k_m z}{k_m^2}=\sum_{m=0}^{\infty}\frac{\cos k_m z}{(2m+1)^2}\,\frac{4d^2}{\pi^2}$$

$$=\left(\frac{2d}{\pi}\right)^2\sum_{m=0}^{\infty}\frac{\cos\left[(2m+1)\frac{\pi z}{2d}\right]}{(2m+1)^2} \qquad (3.3.5)$$

and by summing the series (see eg. Gradshteyn and Ryzhik, 1965, p39) we obtain

$$\sum_{m=0}^{\infty}\frac{\cos k_m z}{k_m^2}=\left(\frac{2d}{\pi}\right)^2\frac{\pi}{4}\left(\frac{\pi}{2}-\frac{\pi z}{2d}\right)$$

(3.3.6)

$$=\frac{d}{2}\,(d-z)$$

Thus (3.3.4) becomes

$$S(-a,z) = i\alpha_1^2(d-z)\,\frac{\sigma_1-\sigma_2}{\sigma_1+\sigma_2} + \sum_{m=0}^{\infty}\left\{k_m F_m^{(2)}(-a) - \frac{2i\alpha_1^2(\sigma_1-\sigma_2)}{dk_m^2(\sigma_1+\sigma_2)}\right\}\cos k_m z \quad .$$

for $y=-a-0$ (3.3.7)

This series should converge rapidly since as 'm' gets large its two terms will cancel each other out. Applying a similar procedure at $y=+a\pm0$ and $y=-a+0$ we obtain the following expressions for the remaining series

$$S(-a,z) = i\alpha_2^2(d-z)\,\frac{\sigma_2-\sigma_1}{\sigma_1+\sigma_2} + \sum_{m=0}^{\infty}\left\{k_m F_m^{(2)}(-a) - \frac{2i\alpha_2^2(\sigma_2-\sigma_1)}{dk_m^2(\sigma_2+\sigma_1)}\right\}\cos k_m z \quad .$$

for $y=-a+0$ (3.3.8)

$$S(a,z) = i\alpha_2^2(d-z)\,\frac{\sigma_2-\sigma_3}{\sigma_2+\sigma_3} + \sum_{m=0}^{\infty}\left\{k_m F_m^{(2)}(a) - \frac{2i\alpha_2^2(\sigma_2-\sigma_3)}{dk_m^2(\sigma_2+\sigma_3)}\right\}\cos k_m z \quad .$$

for $y=+a-0$ (3.3.9)

$$S(a,z) = i\alpha_3^2(d-z)\ \frac{\sigma_3-\sigma_2}{\sigma_3+\sigma_2} + \sum_{m=0}^{\infty}\left\{k_m F_m^{(3)}(a) - \frac{2i\alpha_3^2(\sigma_3-\sigma_2)}{dk_m^2(\sigma_3+\sigma_2)}\right\}\cos k_m z\ .$$

for $y=+a+0$ (3.3.10)

The electric field component V_j/B_0 can now be written as

$$\frac{V_j}{B_0} = -\frac{\omega}{\alpha_j}\sqrt{i}\,\frac{\sinh[(d-z)\alpha_j\sqrt{i}]}{\cosh(d\alpha_j\sqrt{i})} + i\omega(d-z)\ \frac{\sigma_j-\sigma_2}{\sigma_j+\sigma_2}$$

$$+\frac{\omega}{\alpha_j^2}\sum_{m=0}^{\infty}\left\{k_m F_m^{(j)}(y) - \frac{2i\alpha_j^2(\sigma_j-\sigma_2)}{dk_m^2(\sigma_j+\sigma_2)}\right\}\cos k_m z\ .$$

for $i=1,3$ (3.3.11)

$$\frac{V_2}{B_0} = -\frac{\omega}{\alpha_2}\sqrt{i}\,\nu^{(1)} = \left[\nu^{(2)}\right]_{y=-a} + i\omega(d-z)\ \frac{\sigma_2-\sigma_j}{\sigma_2+\sigma_j}$$

$$+\frac{\omega}{\alpha_2^2}\sum_{m=0}^{\infty}\left\{k_m F_m^{(2)}(y) - \frac{2i\alpha_2^2(\sigma_2-\sigma_j)}{dk_m^2(\sigma_2+\sigma_j)}\right\}\cos k_m z\ . \qquad (3.3.12)$$

where, in (3.3.12), j=1 for the y=-a boundary. The

expressions (3.3.11) and (3.3.12) are used instead of (3.2.35) only for calculations at these boundaries.

The advantage of these new expressions (3.3.11) and (3.3.12) is a dramatic decrease in the number of terms in the sum needed to arrive at a final result at $y=\pm a$. For example, at $y=-a$, 14,250 terms are needed when using the original equation (3.2.35) but only 114 terms are needed when using the improved equations. This results in a considerable saving in CPU time.

3.4 Analytic expressions for voltage

Let $v^{(j)}(y;y_0)$ be the voltage between the point $(y,0)$ on the surface of the region with conductivity σ_j $(j=1,2,3)$ and a reference point $(y_0,0)$ anywhere on the surface. According to (2.1.2)

$$v^{(1)}(y;0) = v^{(2)}(-a;0) + \int_{-a}^{y} V^{(1)}\,dy \quad , \tag{3.4.1}$$

$$v^{(2)}(y;0) = \int_{0}^{y} V^{(2)}\,dy \quad , \tag{3.4.2}$$

$$v^{(3)}(y;0) = v^{(2)}(a;0) + \int_{a}^{y} V^{(3)}\,dy \quad . \tag{3.4.3}$$

Integrating the expressions (3.2.35) we obtain

$$v^{(1)}(y;0) = v^{(2)}(-a;0) - \frac{\omega(y+a)\sqrt{i}\,\sinh[(d-z)\alpha_1\sqrt{i}]}{\cosh(d\alpha_1\sqrt{i})}$$

$$+\frac{\omega}{\alpha_1^2}\sum_{m=0}^{\infty}\frac{k_m}{\gamma_m^{(1)}}\left\{F_m^{(1)}(y)-P_m^{(1)}\right\}\cos k_m z\ , \qquad (3.4.4)$$

$$v^{(2)}(y;0) = -\frac{\omega\, y\sqrt{i}\sinh[(d-z)\alpha_2\sqrt{i}]}{\cosh(d\alpha_2\sqrt{i})}+\frac{\omega}{\alpha_2^2}\sum_{m=0}^{\infty}\frac{k_m}{\gamma_m^{(2)}}\left\{L_m^{(3)}\exp[(y-a)\gamma_m^{(2)}]\right.$$

$$\left.-L_m^{(1)}\exp[-(y+a)\gamma_m^{(2)}]\right\}\cos k_m z\ , \qquad (3.4.5)$$

$$v^{(3)}(y;0) = v^{(2)}(a;0) - \frac{\omega(y-a)\sqrt{i}\sinh[(d-z)\alpha_3\sqrt{i}]}{\cosh(d\alpha_3\sqrt{i})}$$

$$-\frac{\omega}{\alpha_3^2}\sum_{m=0}^{\infty}\frac{k_m}{\gamma_m^{(3)}}\left\{F_m^{(3)}(y)-P_m^{(3)}\right\}\cos k_m z\ . \qquad (3.4.6)$$

To obtain the better convergence expressions for the voltages at the boundaries we perform a similar integration on (3.3.11) and (3.3.12) which results in

$$v^{(1)}(y;0) = v^{(2)}(-a;0) - \frac{\omega(y+a)\sqrt{i}\sinh[(d-z)\alpha_1\sqrt{i}]}{\cosh(d\alpha_1\sqrt{i})} + i\omega(y+a)(d-z)\frac{\sigma_1-\sigma_2}{\sigma_1+\sigma_2}$$

$$+\frac{\omega}{\alpha_1^2}\sum_{m=0}^{\infty}\left[\frac{k_m}{\gamma_m^{(1)}}\left\{F_m^{(1)}(y)-P_m^{(1)}\right\}-\frac{2i\alpha_1^2(y+a)}{k_m^2 d}\,\frac{\sigma_1-\sigma_2}{\sigma_1+\sigma_2}\right]\cos k_m z \quad , \quad (3.4.7)$$

$$v^{(2)}(y;0) = -\frac{\omega\, y\sqrt{i}\sinh[(d-z)\alpha_2\sqrt{i}]}{\cosh(d\alpha_2\sqrt{i})}+i\omega y(d-z)\,\frac{\sigma_2-\sigma_j}{\sigma_2+\sigma_j}+\frac{\omega}{\alpha_2^2}\sum_{m=0}^{\infty}\Bigg[\frac{k_m}{\gamma_m^{(2)}}$$

$$\left\{L_m^{(3)}\exp[(y-a)\gamma_m^{(2)}]-L_m^{(1)}\exp[-(y+a)\gamma_m^{(2)}]\right\}-\frac{2iy\alpha_2^2}{k_m^2 d}\,\frac{\sigma_2-\sigma_j}{\sigma_2+\sigma_j}\Bigg]\cos k_m z, \quad (3.4.8)$$

$$v^{(3)}(y;0) = v^{(2)}(a;0) - \frac{\omega(y-a)\sqrt{i}\sinh[(d-z)\alpha_3\sqrt{i}]}{\cosh(d\alpha_3\sqrt{i})}+i\omega(y-a)(d-z)\frac{\sigma_3-\sigma_2}{\sigma_3+\sigma_2}$$

$$-\frac{\omega}{\alpha_3^2}\sum_{m=0}^{\infty}\left[\frac{k_m}{\gamma_m^{(3)}}\left\{F_m^{(3)}(y)-P_m^{(3)}\right\}-\frac{2i\alpha_3^2(y-a)}{k_m^2 d}\,\frac{\sigma_3-\sigma_2}{\sigma_3+\sigma_2}\right]\cos k_m z \quad . \quad (3.4.9)$$

Where for $v^{(2)}(y;0)$ j=1 for the y=-a boundary and j=2 for the y=+a boundary. The voltage between any two points y_j and y_n on the surface of region j and n respectively can be

calculated from the formula

$$v^{(j)}(y_j;y_n) = v^{(j)}(y_j;0) - v^{(n)}(y_n;0) \qquad (3.4.10)$$

The voltage solutions (3.4.4), (3.4.5), and (3.4.6) (with (3.4.7), (3.4.8), (3.4.9) at the conductivity boundaries) were programmed for numerical calculation and the resulting "electric field" values were obtained for the control model shown in Figure 3.2.2.

CHAPTER 4

THE GLOUCESTER FAULT

4.1 The experiment

We now turn to actual field measurements where a line of electrodes is known to traverse a fault: the Gloucester fault in Ontario, Canada. This fault is in the vicinity of Leitrim, near Ottawa, and strikes roughly southeast for nearly 50 km. The geology of the region is shown in Figure 4.1.1 (Telford et al.,1977). Beds of Carlsbad shale form the north side of the contact, adjoining Oxford limestones in the northwest half, while March and Nepean sandstones occupy the southeast portion (Wilson,1946). The resistivities of the various formations are from Telford et al. (1977) with the exception of those values in brackets which were assumed on the basis of known resistivities for formations of similar composition (Jones,1986). The field data from the Gloucester fault shown in Figure 4.1.2 (Jones,1986) illustrate dramatically the large attenuation of electric fields between sites only

Figure 4.1.1 Geology and apparent conductivities of the Gloucester Fault. Conductivities are from Telford et al. (1977) except for those in brackets which are assumed on the basis of conductivities for similar rock types in the area.

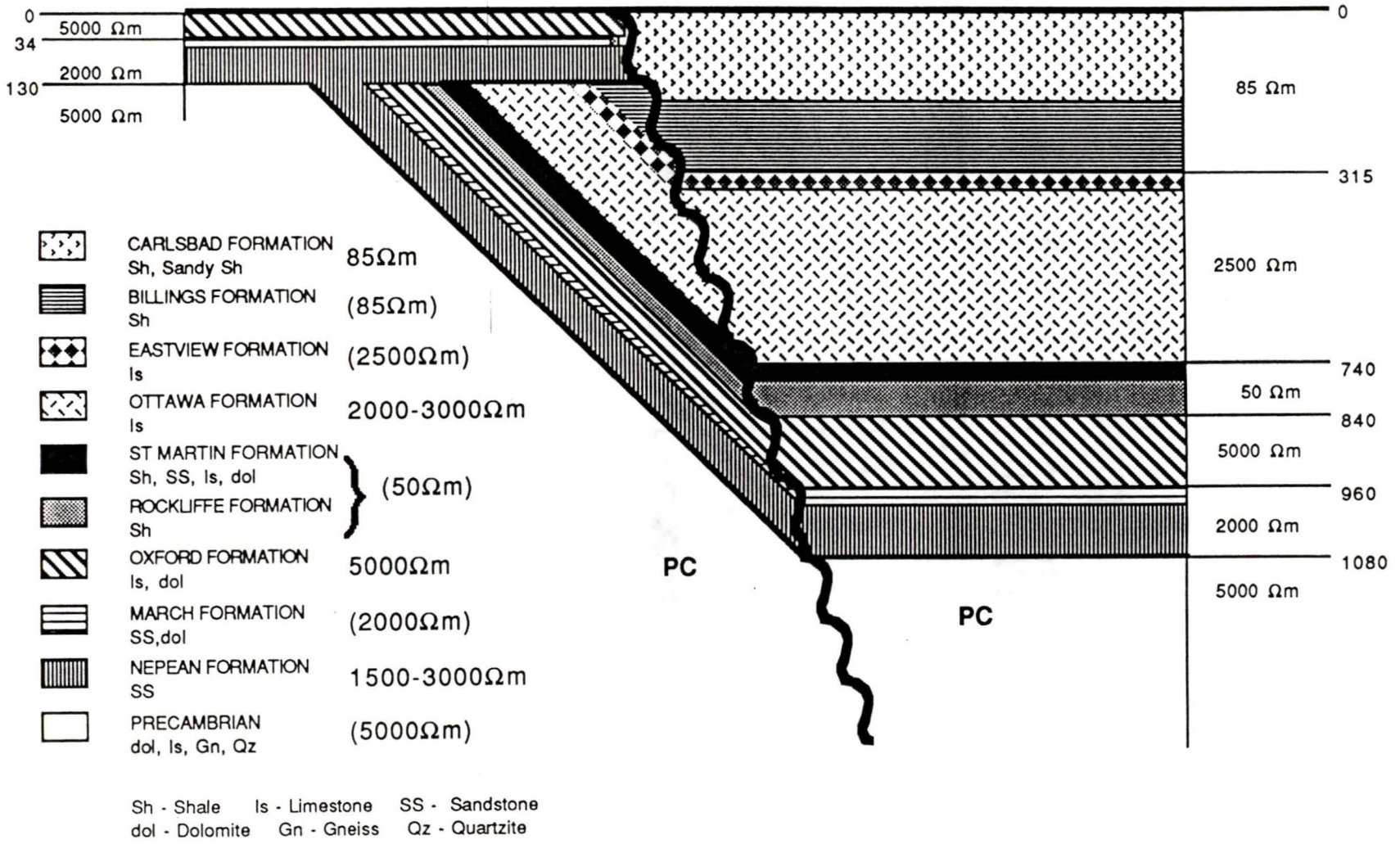

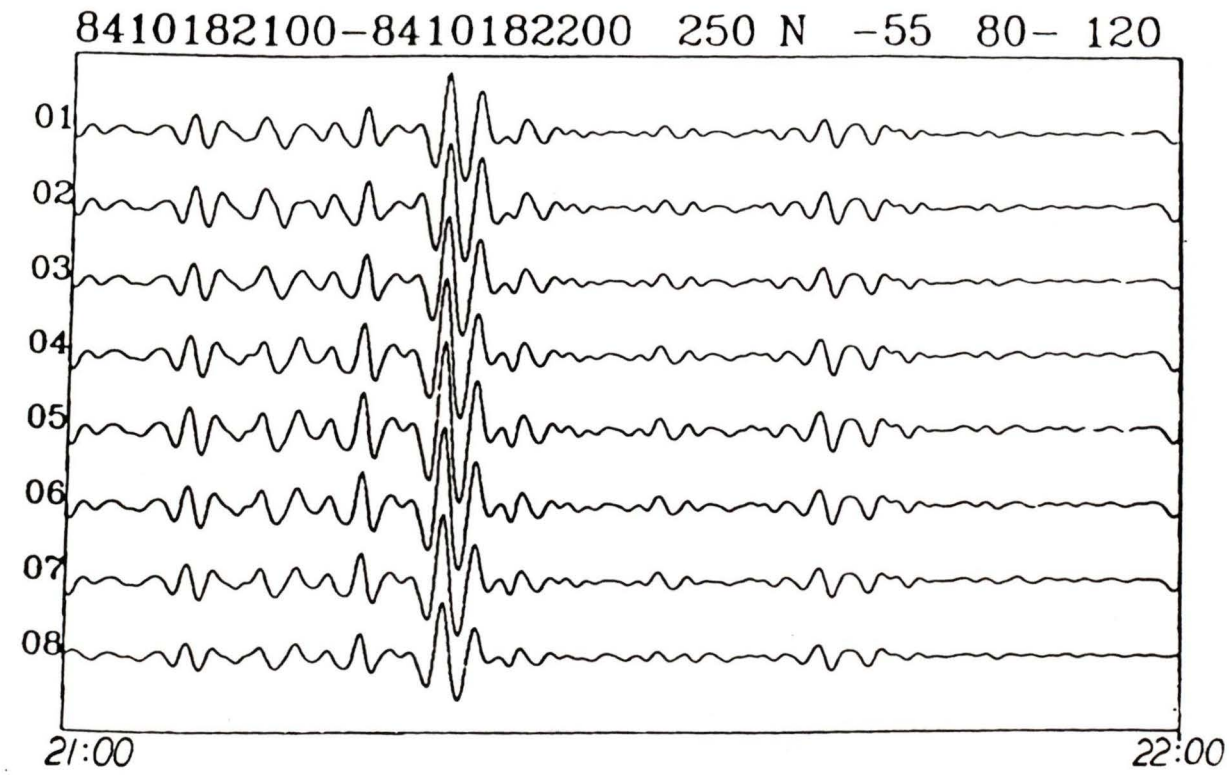

Electric fields parallel to the fault

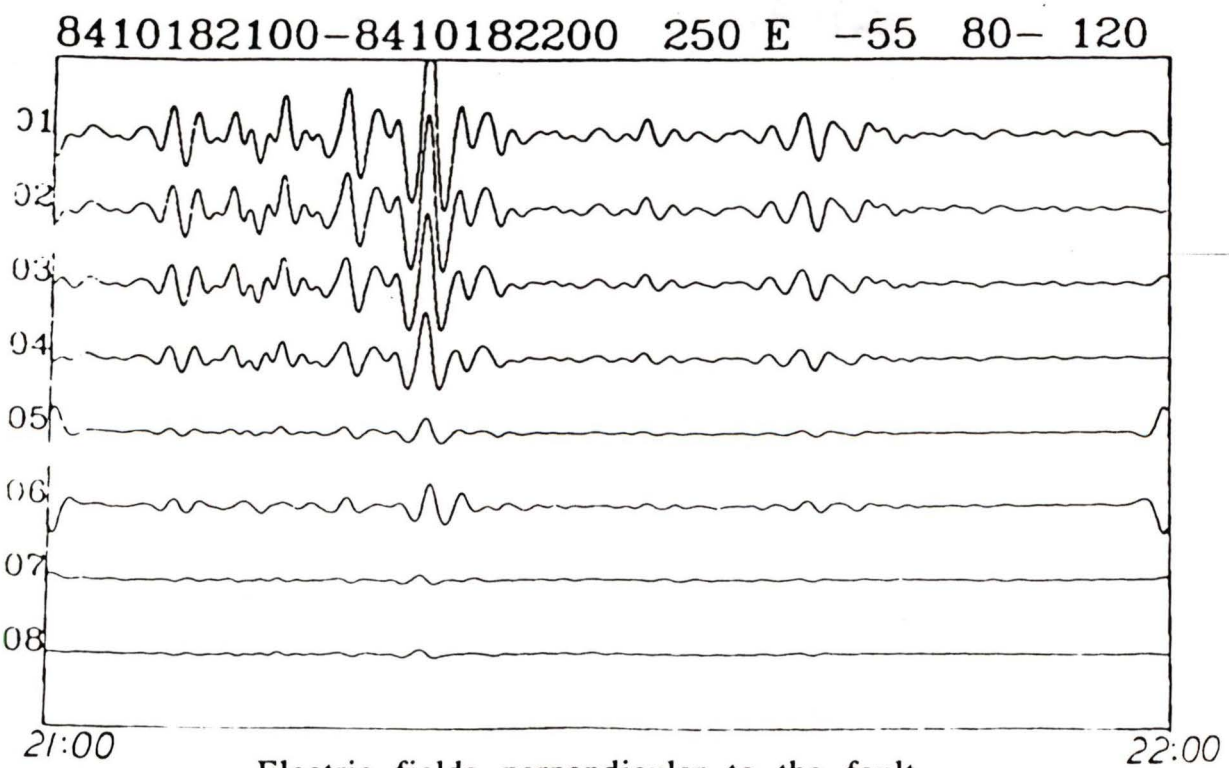

Electric fields perpendicular to the fault

Figure 4.1.2 Electric field data from the Goucester fault, Ontario, Canada.

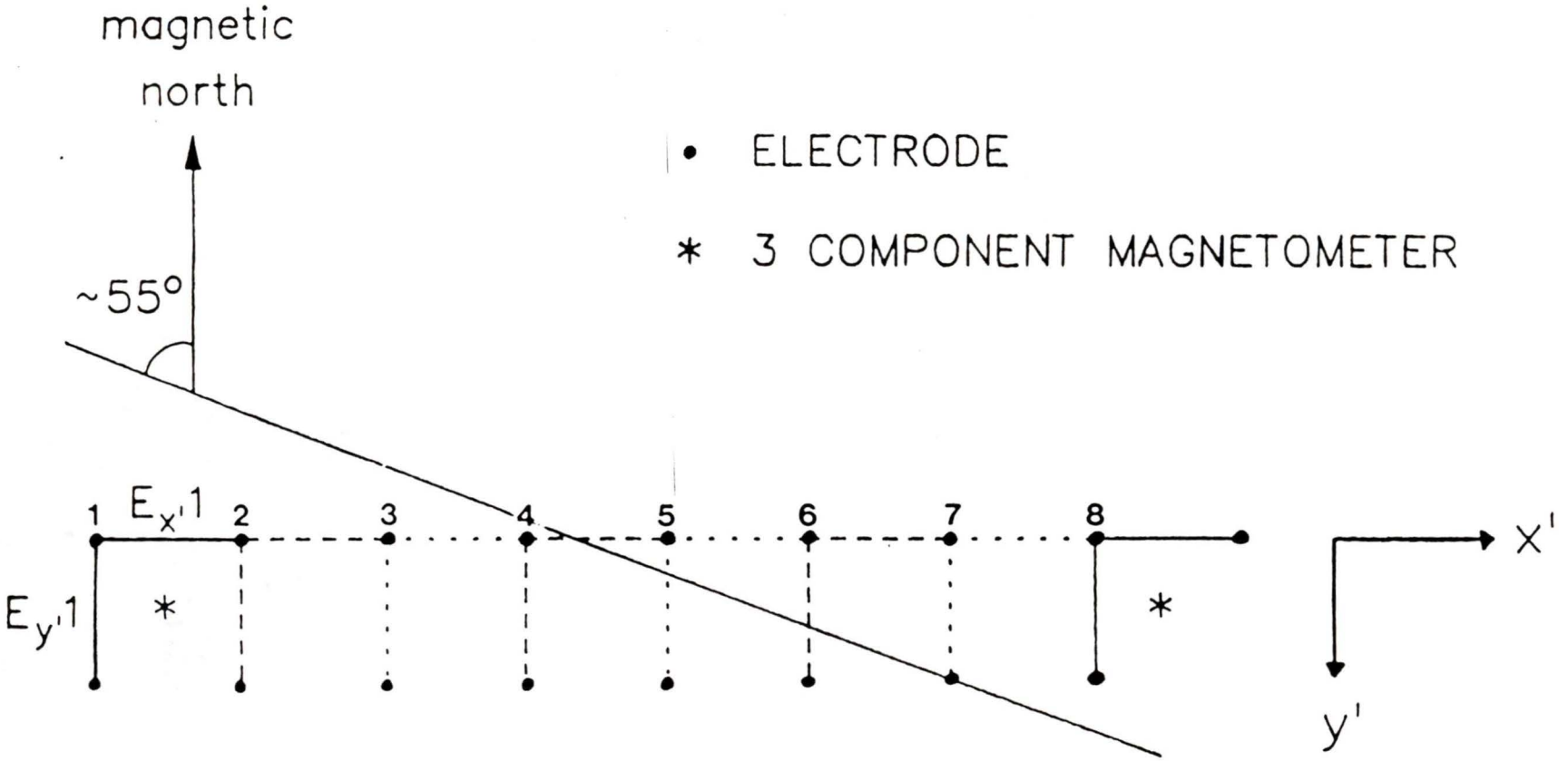

Figure 4.1.3 Orientation and position of the electrode profile in the Gloucester fault area.

50 m apart. Obviously this is a case where equation (2.1.1) will not be valid for the electrode pair straddling the fault. The profile of electrodes is shown in Figure 4.1.3 (Jones,1986). The electric fields in the two perpendicular directions are given by the measured voltages divided by their separation and are assigned to the left hand electrodes 1 through 8. Magnetic recordings were taken by PHOENIX magnetometers at the centre of the squares associated with electrodes 1 and 8. Since the fields we want to study are the fields perpendicular and parallel to the strike and not those along the (x',y') axes defined by the electrode pairs, we must first perform a transformation.

4.2 Transformation of finite difference voltages to fault coordinate system

The notation used for the transformation of the fields from the profile coordinate system to the fault coordinate system is shown in Figure 4.2.1 The electrode stations are labelled in ascending order along the x'-axis in the direction of increasing x'. Thus the m^{th} station has coordinates $(x_m', 0)$ in the primed coordinate system and the transverse station at the m^{th} point has coordinates (x_m', d_m^y) where $d_m^y = y_m' - 0$ is the separation of the electrodes. The separation of electrodes along the x'-axis is $d_m^y = x_{m+1} - x_m$. Now the m^{th} station, $(x_m', 0)$, has coordinates (x_{2m}, y_{2m}) in the unprimed coordinate system and the corresponding transverse station at (x_m', d_m^y) has coordinates (x_{2m+1}, y_{2m-3}). This notation holds only for strike angles α less than $\pi/4$. For example when $\alpha > \pi/4$ $(x_m', 0)$ maps into (x_{2m}, y_{2m}) but the transverse station (x_m', d_m^y) maps into (x_{2m+3}, y_{2m-1}). Note that in both cases

the points y_n along the y-axis correspond to the stations on the profile when n is even and to the transverse stations when n is odd. On the Gloucester fault the electrodes were aligned with $\alpha=35^{\circ}$. The equations of transformation are clearly

$$x'=-x\cos\alpha + y\sin\alpha,$$

$$y'=-x\sin\alpha - y\cos\alpha, \tag{4.2.1}$$

and

$$x=-x'\cos\alpha - y'\sin\alpha,$$

$$y=x'\sin\alpha - y'\cos\alpha. \tag{4.2.2}$$

Likewise the horizontal electric field components on the surface z=0 satisfy the same transformation equations (4.2.1), and (4.2.2) and since the B-polarization field has, by definition, U(y)=0 (since $\underline{E}=(0,V,W)$) the horizontal components U',V', in the electrode (primed coordinate system are given by

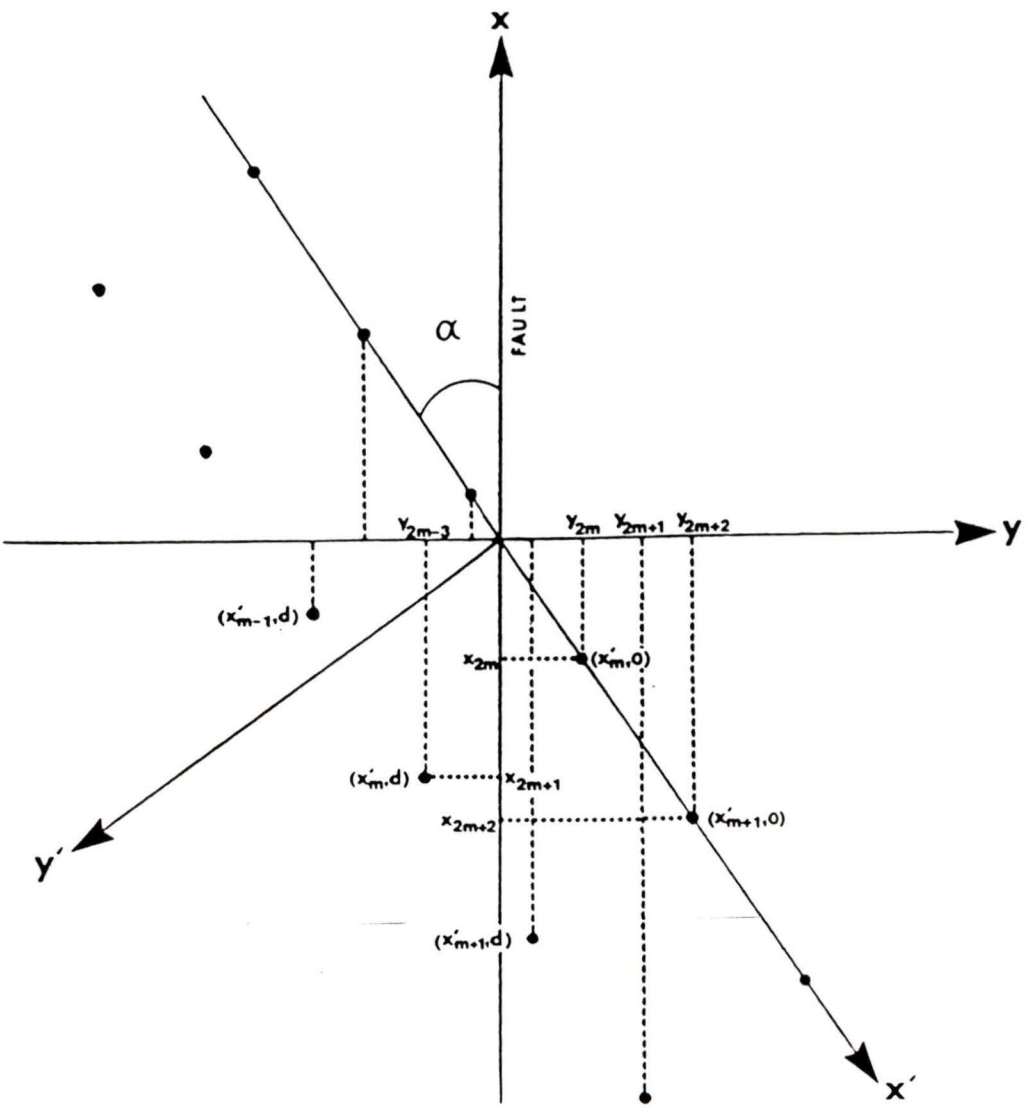

Figure 4.2.1 Notation used in the numerical program to transform the electric fields along the electrode profile to fields perpendicular and parallel to the strike.

$$U'(x',y')=V(y)\sin\alpha,$$

$$V'(x',y')=-V(y)\cos\alpha, \tag{4.2.3}$$

and

$$U(y)=0\ ,$$

$$V(y)=U'(x',y')\sin\alpha - V'(x',y')\cos\alpha. \tag{4.2.4}$$

where for convenience we have dropped all z-dependencies. The components U_m', V_m', at station m are measured in the field as

$$\tilde{V}_m' = \frac{\nu(x_m', d_m^y; x_m', 0)}{d_m^y} \tag{4.2.5}$$

$$\tilde{U}_m' = \frac{\nu(x_{m+1}', 0; x_m', 0)}{d_m^x} \tag{4.2.6}$$

where $\nu(x_1', y_1'; x_2', y_2')$ is the voltage measured along the

straight line between (x_1', y_1') and (x_2', y_2') and where the tilda denotes an electric field given by voltage divided by separation distance. By equations (2.1.1) and (2.1.2) we obtain

$$\tilde{U}_m' = \frac{1}{d_m^x} \int_{x_m'}^{x_{m+1}'} U'(x', 0)\, dx' \ ,$$

$$\tilde{V}_m' = \frac{1}{d_m^y} \int_{0}^{d_m^y} V'(x_m', y')\, dy' \ . \qquad (4.2.7)$$

We can transform the integrals (4.2.7) into the unprimed coordinate system by using equations (4.2.1), (4.2.2) and definitions (4.2.3), (4.2.4) which give

$$\tilde{U}_m' = \frac{1}{d_m^x} \int_{y_{2m}}^{y_{2m+2}} V(y)\, dy \ , \qquad \tilde{V}_m' = \frac{1}{d_m^y} \int_{y_{2m}}^{y_{2m-3}} V(y)\, dy \ . \qquad (4.2.8)$$

Now $y_{2m+2} = y_{2m} + d\sin\alpha$ and $y_{2m-3} = y_{2m} - d\cos\alpha$ and by analogy with (4.2.1), and (4.2.2) we have

$$\tilde{U}_m = -\tilde{U}_m' \cos\alpha - \tilde{V}_m' \sin\alpha \quad ,$$

$$\tilde{V}_m = \tilde{U}_m' \sin\alpha - \tilde{V}_m' \cos\alpha \quad , \qquad (4.2.9)$$

which, combined with (4.2.8), give

$$\tilde{U}_m = \frac{\sin\alpha}{d_m^x} \int_{y_{2m}-d\cos\alpha}^{y_{2m}} V(y)\,dy - \frac{\cos\alpha}{d_m^x} \int_{y_{2m}}^{y_{2m}+d\sin\alpha} V(y)\,dy \quad , \qquad (4.2.10)$$

$$\tilde{V}_m = \frac{\cos\alpha}{d_m^y} \int_{y_{2m}-d\cos\alpha}^{y_{2m}} V(y)\,dy + \frac{\sin\alpha}{d_m^y} \int_{y_{2m}}^{y_{2m}+d\sin\alpha} V(y)\,dy \quad . \qquad (4.2.11)$$

It is interesting to note that even though we started with a two-dimensional B-polarization model in which U=0, the use of voltages to calculate electric fields has introduced a spurious electric field $\tilde{U}$. This would disappear, of course, if the electrode profile were aligned perpendicularly to the fault (ie. if $\alpha=\pi/2$).

4.3 The two-dimensional model

An idealized two-dimensional B-polarizaion model for numerical modelling of the Gloucester fault is shown in Figure 4.3.1 (Jones,1986). The model is a rough representation of a cross-section through the fault zone and approximates the assumed geology shown in Figure 4.1.1 The different strata on each side of the fault are supported by a layer of precambrian rock with a resistivity of 5000 Ω-m. This is underlain by an infinite conductor at a depth of 35 km. This model was used in the finite difference program to obtain both the true electric field and the "electric field" from voltages for a period of 100 seconds.

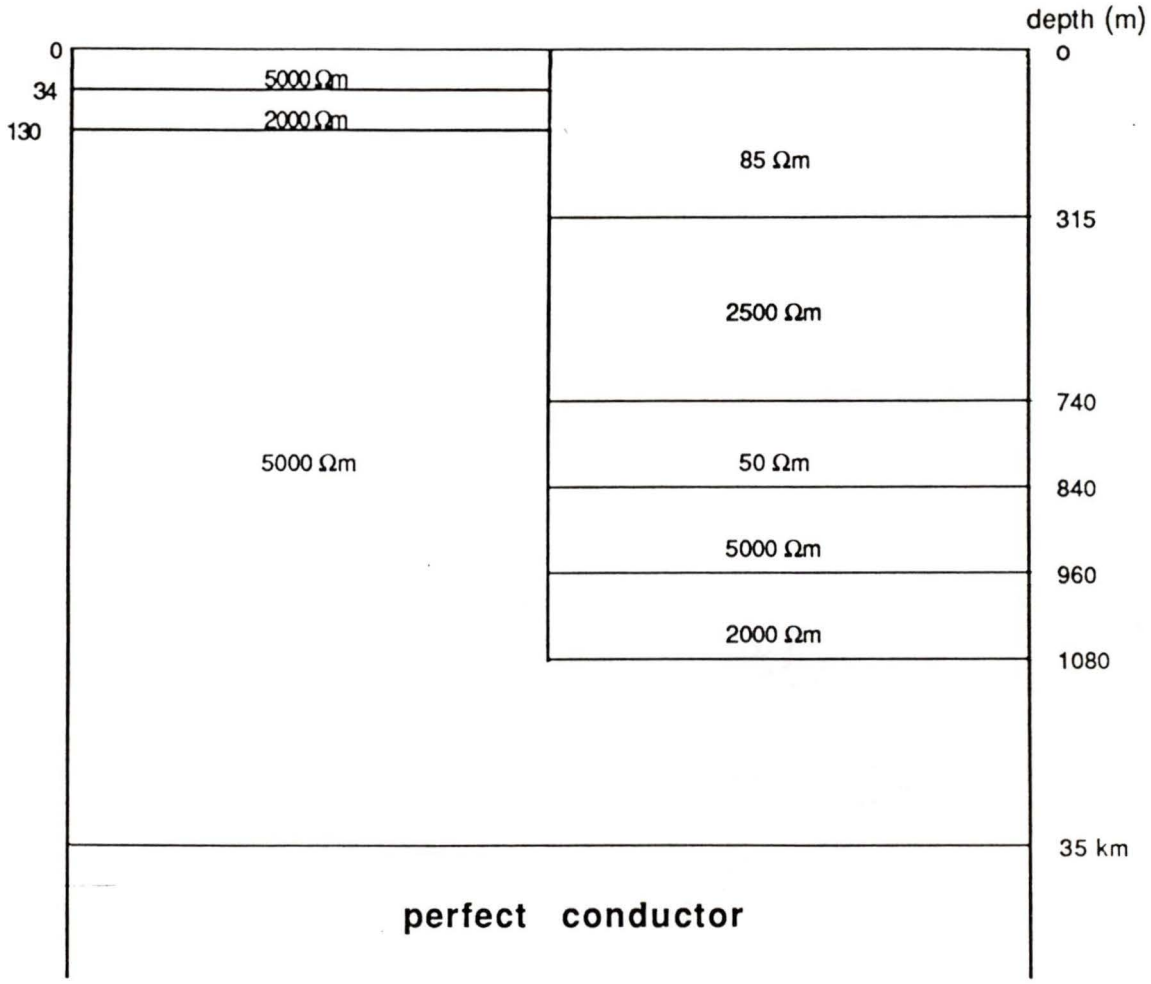

Figure 4.3.1 An idealized model of the Gloucester fault used in the numerical calculations.

CHAPTER 5

RESULTS AND DISCUSSION

5.1 Comparison with analytic model

In order to establish the accuracy of our finite difference calculation of voltages we must compare them to the analytic voltage solutions for the control model illustrated in Figure 3.2. The model parameters used were $T=2\pi/\omega=300s$, $a=10km$, $d=50km$, $\sigma_1=0.1$ S/m, $\sigma_2=1.0$ S/m and $\sigma_3=0.5$ S/m. In Figure 5.1.1 and 5.1.2 and in Table 5.1.1 the analytic values for the true electric field and the corresponding analytic and numerical values obtained from voltage differences are compared. The excellent agreement between the two voltage fields illustrates the accuracy of our finite difference expression for voltages. It is clear, however, that the "electric field" given by voltage divided by separation distance is only an approximation to the true electric field. Away from conductivity boundaries the two methods of calculation give the same results but on and near the boundaries there is considerable error in

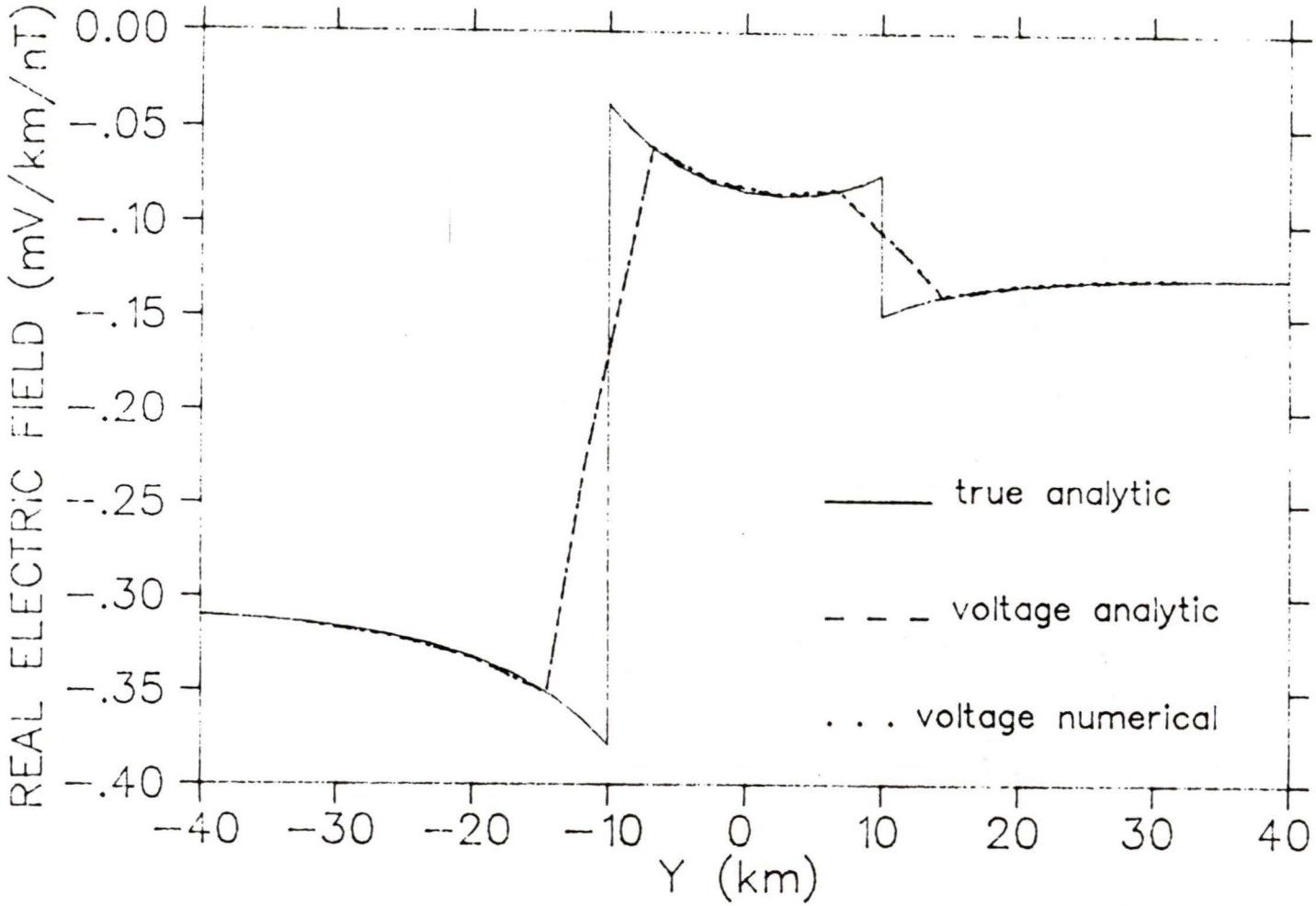

Figure 5.1.1 A graphical comparison of the real true electric field and the corresponding values obtained from voltage divided by separation distance. Note that analytic and numerical voltage electric field values are so close as to be indistinguishable on the graph.

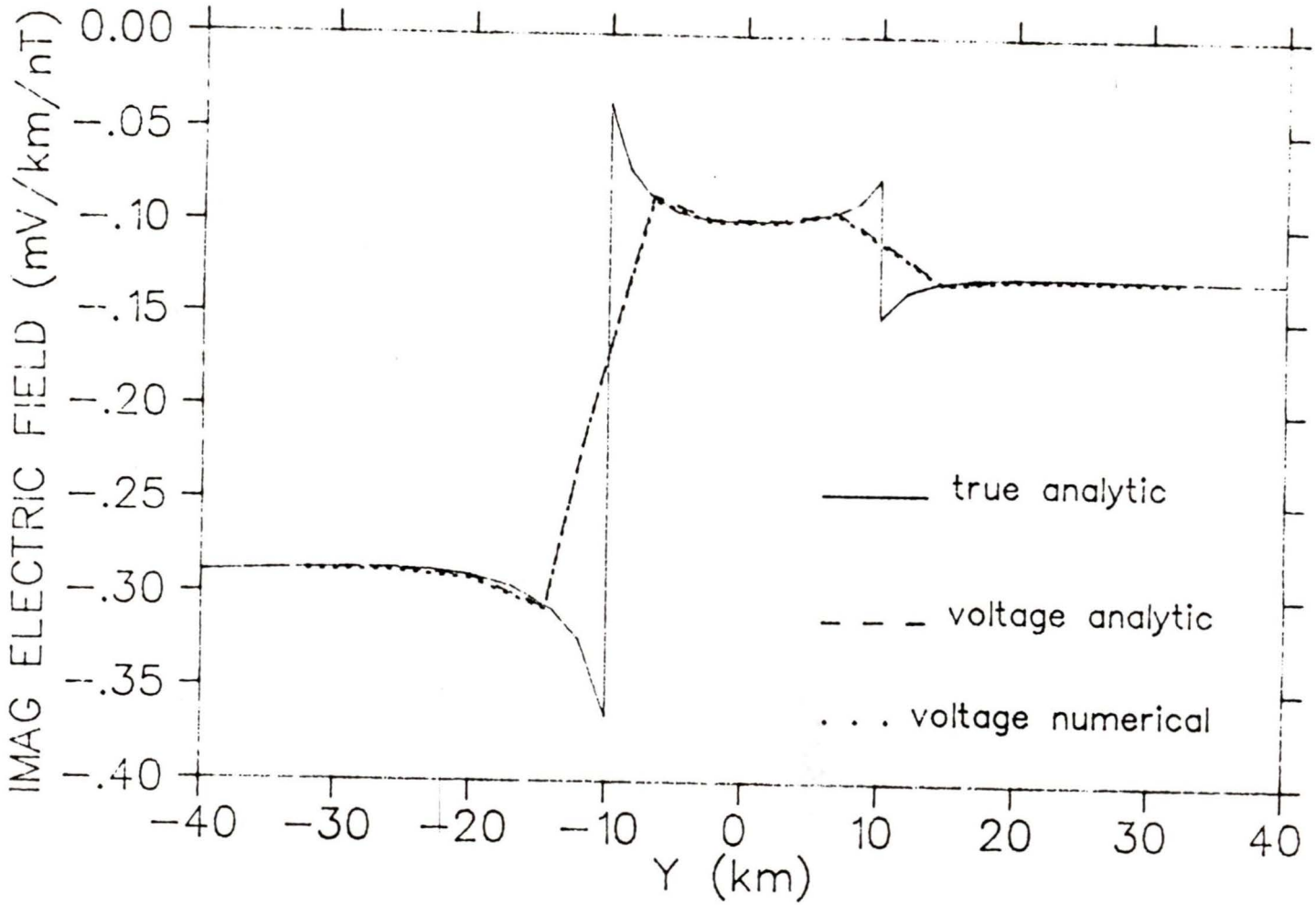

Figure 5.1.2 A graphical comparison of the imaginary true electric field and the corresponding values obtained from voltage divided by separation distance. Note that analytic and numerical voltage electric field values are so close as to be indistinguishable on the graph.

TABLE 5.1

Comparison of the true electric field with the analytic and numerical voltage electric field in the y-direction (mV/km/nT). The voltage fields were assigned to a point midway between the two points which provided the voltage used in each calculation.

Model parameters: a=10.0 km, d=50.0 km, T=300.0 s, σ_1=0.10 S/m σ_2=1.00 S/m, σ_3=0.50 S/m.

			Voltage Divided by Separation Distance			
y(km)	True Analytic		Analytic		Numerical	
	real	imag	real	imag	real	imag
-35.000	-.3122	-.2879				
-32.000	-.3142	-.2873	-.3143	-.2873	-.3143	-.2884
-29.000	-.3168	-.2869				
-26.000	-.3204	-.2870	-.3206	-.2871	-.3206	-.2883
-23.000	-.3252	-.2880				
-20.000	-.3317	-.2906	-.3321	-.2911	-.3321	-.2922
-17.000	-.3406	-.2962				
-14.500	-.3507	-.3055	-.3512	-.3070	-.3510	-.3080
-12.000	-.3641	-.3244				
-11.750	-.3657	-.3273	-.2308	-.2191	-.2304	-.2189
-10.000	-.3786	-.3658				
-10.000	-.0378	-.0365				
-8.500	-.0495	-.0712				
-6.750	-.0608	-.0866	-.0604	-.0853	-.0601	-.0877
-5.000	-.0696	-.0940				
-2.500	-.0783	-.0982	-.0777	-.0977	-.0772	-.0990
0.000	-.0834	-.0990				
2.500	-.0854	-.0982	-.0849	-.0980	-.0843	-.0992
5.000	-.0846	-.0961				
6.750	-.0825	-.0933	-.0823	-.0929	-.0817	-.0942
8.500	-.0789	-.0879				
10.000	-.0745	-.0752				
10.000	-.1491	-.1505				
11.750	-.1440	-.1368	-.1164	-.1163	-.1156	-.1175
12.000	-.1434	-.1358				
14.500	-.1385	-.1304	-.1387	-.1309	-.1380	-.1315
17.000	-.1352	-.1283				
20.000	-.1326	-.1275	-.1327	-.1276	-.1321	-.1286
23.000	-.1309	-.1275				
26.000	-.1300	-.1278	-.1300	-.1278	-.1294	-.1288
29.000	-.1294	-.1281				
32.000	-.1291	-.1284	-.1291	-.1284	-.1285	-.1294
35.000	-.1289	-.1286				

estimating electric fields by voltage calculations.

In the above conparison the "electric field" was assigned to a point midway between the two electrodes measuring the voltage. It can be seen from Table 5.1.1 that this results in a more accurate respresentation of the field than if the electric field value were assigned to one of the two electrode positions. Unfortunately this latter course of action is followed in most experimental studies.

5.2 Comparison with Gloucester fault data

As a final illustration of the method developed in this thesis we present a simple comparison of the electric fields shown in Figure 4.1.2. The fields obtained from these data were first filtered with a bandwidth of 90-110s, and then fitted with a sine wave of 100s period whose peak value occurred at time 21:20:10. The adjacent troughs of the sine wave were at 21:19:15 and 21:21:00. In Table 5.2.1 the values of the field at these points and the resulting full range (trough to peak) amplitude for each station are listed in mV/km. In Table 5.2.2 these full range variations of the electric field (ie. twice the amplitude of the sine wave) are compared with the corresponding values given by our true electric field and voltage calculations. These latter values were normalized by the measured values at Station 1 (as far removed from the fault as possible) before tabulation. Also shown are the values of the component of electric field (similarly normalized) parallel to the fault given by the voltage

TABLE 5.2.1

Field values: magnitude of 100s sinusoid which maximizes at 21:20:10 in mV/km

Station	minimum 19:15	maximum 20:10	minimum 21:00	amplitude
1	-25.2	41.9	-28.3	68.7
2	-22.3	35.6	-22.9	58.2
3	-17.5	26.9	-17.4	44.4
4	-11.4	17.5	-11.6	29.0
5	-3.52	5.95	-4.09	9.76
6*	-5.51	8.90	-6.79	15.1
7	-1.29	2.07	-1.53	3.48
8	-1.21	1.85	-1.29	3.10

* 15-20s delay, believed to be instrument problem.

Station	experimental $\lvert E_{\perp} \rvert$	true $\lvert E_{\perp} \rvert$	voltage divided by separation distance $\lvert E_{\perp} \rvert$	voltage divided by separation distance $\lvert E_{\parallel} \rvert$
1	68.7	68.7	68.7	0.31
2	58.2	69.3	69.1	0.31
3	44.4	69.9	69.8	0.38
4*	29.0	70.8	52.2	25.7
5	9.76	1.82	22.1	14.1
6	15.1	2.19	2.05	0.17
7	3.48	2.36	2.28	0.08
8	3.10	2.43	2.27	0.14

* 15-20s delay believed to be instrument problem

Table 5.2.2 A comparison of electric field amplitudes in mV/km.

calculation in (4.2.10).

It can be seen from Table 5.2.2 that neither the calculated true electric field nor the voltage computation are in remarkably close agreement with the measured field values in the region of the fault. However, the results given by voltage divided by separation distance clearly represent a better approximation to the observed behavior of the measured electric field than the computed value of the true electric field, particularly at Station 4. The latter actually increases slightly between Stations 3 and 4 whereas the amplitude of the observed field shows a steep decline from Stations 3 to 5. This decline is much more faithfully reproduced by the voltage difference calculations. The spurious electric field parallel to the fault shown in column 5 of Table 5.2.2 is surprisingly large at Stations 4 and 5 (49% and 64% respectively of the corresponding fields perpendicular to the fault), thereby revealing another source of error inherent in field measurements involving the magnetotelluric method. It is to be expected that an E-polarization field will contribute in a similar manner to the field measured by voltages

perpendicular to the fault, but no attempt has been made in this study to estimate the contribution from an E-polarization field to the total amplitude of the perpendicular electric field in the neighbourhood of the fault.

5.3 Conclusion

In this thesis a method has been developed for modifying existing analytic and finite difference programs so that they are capable of calculating voltage difference electric fields. The expressions for voltage obtained in chapter 2 have the same degree of accuracy (up to second order terms) as the electric fields obtained from the finite difference program of Brewitt-Taylor and Weaver (1976) to which the voltage modifications were made. In section 5.1 it has been shown that the accuracy of these results is excellent when compared to the suitably modified analytical solution of Weaver, Le Quang and Fischer (1985). It is also shown here that the location (left-hand electrode, right-hand electrode or halfway between) to which the "electric field" is assigned is critical for an accurate comparison of data. It is observed that assigning the field to a position inbetween the two nodes or electrodes used in the voltage difference calculation yields the best results.

Also noteworthy is the appearence of a spurious electric field parallel to the fault which arises in voltage difference calculations when the electrode profile is not perpendicular to the fault. This error appears to be quite large and inherent in the method used.

In the magnetotelluric method comparisons are usually made between apparent resistivity and phase, but both of these parameters are, of course, affected by the electric field values. The main pupose of this thesis is to draw attention to possible sources of error in the interpretation of measured apparent resistivity and phase values when comparing them with model calculations in regions where the electrode profile crosses a geological fault. In particular it is recommended that model calculations use voltage differences to compute the electric fields for comparison with real data.

REFERENCES

Ashour, A.A., 1971. Electromagnetic induction in thin finite sheets having conductivity decreasing to zero at the edge, with geomagnetic applications.-I. Geophys. J. R. astr. Soc., **8**, 375-388.

Brewitt-Taylor, C.R., and Weaver, J.T., 1976. On the finite difference solution of two-dimensional induction problems. Geophys. J. R. astr. Soc., **47**, 375-396.

Cagniard, L. 1953. Basic theory of the magneto-telluric method of geophysical prospecting. Geophysics, **18**, 605-635.

Dawson, T.W., 1979. Three-dimensional electromagnetic induction inthin sheets. Ph.D. Thesis, University of Victoria, Victoria, B.C.

Dawson, T.W., and Weaver, J.T., 1979. H-polarization induction in two thin half-sheets. Geophys. J. R. astr. Soc., **56**, 419-438.

Dawson, T.W., Weaver, J.T., and Raval, U., 1982. B-polarization induction in two generalized thin sheets at the surface of a conducting half-space. Geophys. J. R. astr. Soc., **69**, 209-234.

Dosso, H.W., 1973. A review of analogue model studies of the coast effect. Phys. Earth Planet. Interior, **7**, 294-302.

D'Erceville, I., and Kunetz, G., 1962. The effect of a fault on the earth's electromagnetic field. Geophysics, **27**, 651-665.

Fischer, G., Le Quang, B.V., and Müller, I., 1983. VLF ground surveys, a powerful tool the study of shallow two-dimensional structures. Geophysical Prospecting, **31**, 977-991.

Geyer, R.G., 1972. The effect of dipping contact on the behavior of the electromagnetic field. Geophysics, **37**, 337-350.

Gradshteyn, I.S., and Ryzhik, I.M., 1965. Table of Integrals, Series, and Products. Academic Press, New York.

Green, R., 1978. The Two-Dimensional Theory of Electromagnetic Induction in Thin Sheets With Applications to the Earth. M.Sc. Thesis, University of Victoria, Victoria, B.C.

Jackson, J.D., 1975. Classical Electrodynamics, 2nd ed. John Wiley and Sons Inc., New York.

Jones, A.G., 1986. private communication.

Jones, D.S., 1964. The Theory of Electromagnetism. Pergamon Press, Oxford.

Kaufman, A.A., and Keller, G.V., 1981. The Magnetotelluric Sounding Method. Elsevier Scientific Pub. Co., New York.

Moon, P., and Spencer, D.E., 1960. Foundations of Electrodynamics. D. Van Nostrand Company Inc., Princeton.

Nicoll, M.A., and Weaver, J.T., 1977. H-polarization induction over an ocean edge coupled to the mantle by a conductive crust. Geophys. J. R. astr. Soc., **49**, 427-442.

Price, A.T., 1949. The induction of electrical currents in non-uniform thin sheets and shells. Quant. J. Mech. Appl. Math., **2**, 283-310.

Price, A.T., 1950. Electromagnetic induction in a semi-infinite conductor with a plane boundary. Quart. J. Mech. Appl. Math., **3**, 385-410.

Rankin, D., 1962. The magneto-telluric effect on a dike. Geophysics, **27**, 666-676.

Rikitake, T., 1966. Electromagnetism and the Earth's Interior. Elsevier Publishing Co., Amsterdam.

Rikitake, T., 1973. Global electrical conductivity of the earth. Phys. Earth Planet. Inter., **7**, 245-250.

Roden, R.B., 1964. The effect of an ocean on magnetic diurnal variations. Geophys. J. R. astr. Soc., **8**, 375-388.

Telford, W.M., King, W.F., and Becker, A., 1976. VLF mapping of geological structure. Geol. Surv. Can., Paper 76-25.

Wait, J.R., 1954. On the relation between telluric currents and the Earth's magnetic field. Geophysics, **19**, 281-289.

Wait, J.R., 1962. Theory of magnetotelluric fields. J. Res. Natl. Bur. Std., D., **66(5)**, 509-541.

Wait, J.R., and Spies, K.P., 1974. Magneto-telluric fields for a segmented overburden. J. Geomag. Geoelectr., **26**, 449-458.

Wait, J.R., 1982. Geo-electromagnetism. pp 197-201, Academic Press, New York.

Wannemaker, P.E., Stodt, J.A., and Rijo, L., 1987. A stable finite element solution for two-dimensional magnetotelluric modelling. Geophys. J. R. astr. Soc., **88**, 277-296.

Ward., S.H., Peeples, W.J., and Ryu, U., 1973. Analysis of geomagnetic data. Methods in computational physics, **13**, 163-238, ed. Bruce A. Bolt, Academic Press, New York.

Weaver, J.T., 1963. The electromagnetic field within a discontinuous conductor with reference to geomagnetic micropulsations near a coastline. Can. J. Phys., **41**, 484-495.

Weaver, J.T., 1971. The general theory of electromagnetic induction in a conducting half-space. Geophys. J. R. astr. Soc., **22**, 83-100.

Weaver, J.T., Le Quang, B.V., and Fischer, G., 1985. A comparison of analytical and numerical results for a two-dimensional control model in electromagnetic induction. Geophys. J. R. astr. Soc., **82**, 263-278.

Weidelt, P., 1971. The electromagnetic induction in two thin half-sheets. Z. Geophys., **37**, 649-665.

Wilson, A.E., 1946. Geology of the Ottawa-St. Lawrence lowlands, Ontario and Quebec. Geol. Surv. Can., Mem. 241.

APPENDIX A

PROGRAM LISTINGS

This appendix contains the Fortran programs for the improved convergence analytic caculation of the true and voltage electric fields. As near as possible the program follows the notation introduced in this thesis. The numerical voltage calculations are modifications of the numerical modelling program of Brewitt-Taylor and Weaver (1976). Since this program is too long to be listed here only the subroutines pertaining to the voltage calculations are included. Subroutines for calculation of the voltage at both the right and left-hand side of a grid node appear as well as a listing for the program which calculates the field components for electrode profiles not perpendicular to the fault.

```
      PROGRAM BPOL
C
C  VERSION 20-MAR-1984 (AMENDED MAY 1986)  WRITTEN BY WEAVER
C  ************************** MAIN ***********************************
C    A B-POLARIZATION CALCULATION IN ELECTROMAGNETIC INDUCTION
C  THIS PROGRAM COMPUTES THE ELECTROMAGNETIC FIELD INDUCED IN A
C  SEGMENTED CONDUCTING SLAB BY A UNIFORM HORIZONTAL MAGNETIC FIELD.
C  THE MODEL CONSISTS OF A SLAB OF THICKNESS "D" UNDERLAIN BY A PERFECT
C  CONDUCTOR AT DEPTH Z=D.  THE SLAB IS DIVIDED INTO 3 SEGMENTS :
C     (1) Y.LT.-A OF CONDUCTIVITY SIGMA(1) .
C     (2) Y BETWEEN -A AND A OF CONDUCTIVITY SIGMA(2).
C     (3) Y.GT.+A OF CONDUCTIVITY SIGMA(3).
C  THE INDUCING MAGNETIC FIELD IS UNIFORM IN THE X-DIRECTION AND HAS
C  A PERIOD "T" SPECIFIED BY THE USER.  VACUUM PERMEABILITY IS ASSUMED
C  EVERYWHERE.  THE PROGRAM COMPUTES THE TOTAL MAGNETIC FIELD BX
C  (X-COMPONENT OF THE MAGNETIC FIELD) PLUS EY AND EZ (Y- AND Z-
C  COMPONENTS OF THE ELECTRIC FIELD) AT THE ARRAY OF POINTS (Y,Z)
C  DEFINED BY GIVEN VALUES OF Y AND Z.  THE FIELD COMPONENTS ARE
C  NORMALIZED BY THE CONSTANT EXTERNAL MAGNETIC FIELD.  IF NORMALISATION
C  OF THE ELECTRIC FIELD BY ITS SURFACE VALUE AT Y = -INFINITY IS
C  DESIRED (E.G. AS IN THE COMMEMI PROJECT) THEN THE FINAL TWO
C  STATEMENTS IN SUBROUTINE SERIES, NAMELY cv=cv/cnorm AND cw=cw/cnorm,
C  SHOULD HAVE THEIR COMMENT CHARACTERS C IN COLUMN 1 REMOVED.
C
C  INPUT DATA TO BE PROVIDED BY THE USER SHOULD BE IN FREE FORMAT IN
C  FOR005 :  (1) A : HALF-WIDTH IN KM OF THE MIDDLE SEGMENT.
C            (2) D : THICKNESS OF THE SLAB IN KM.
C            (3) SIGMA(3) : ARRAY CONTAINING CONDUCTIVITY VALUES IN S/M
C            (4) T : PERIOD OF FIELD, IN SECONDS.
C            (5) SMALL : CONTROL PARAMETER FOR ACCURACY.
C            (6) NY AND YY : THE NUMBER OF HORIZONTAL POINTS Y AT WHICH
C                     THE FIELD IS REQUIRED, AND THEIR COORDINATES
C            (7) NZ AND ZZ : THE NUMBER OF VERTICAL POINTS Z AND
C                     THEIR COORDINATES
C  THE CONTROL PARAMETER "SMALL" MAY BE CHANGED TO PROVIDE QUICKER
C  (LESS ACCURATE) CALCULATIONS.  NORMALLY SMALL = 1.0D-8
C  RESULTS ARE WRITTEN TO FOR006
C  SUBROUTINES USED : SERIES  -  SIDE  -  MIDDLE
C
C  DEFINE VARIABLE TYPES
C
      IMPLICIT      REAL*8 (A,B,D,E,G,H,O-Z),
     1              COMPLEX*16 (C),
     2              LOGICAL*1 (F)
      COMPLEX*16 CGAMMA(3),CBETA(2),CK(2)
      REAL*8        YY(200),ZZ(50),SIGMA(3),ALPHA(3)
      COMMON        ONE,TWO,CI,A,D,OMEGA,cnorm
C
C  DEFINE CONSTANTS
C
      PARAMETER (THOU=1.0D3,PI=3.14159265358979323D0)
      PARAMETER (RMU=PI*4.0D-7,CO=(0.0D0,0.0D0))
C
C  MODEL PARAMETERS
C
      ONE=1.0D0
      TWO=2.0D0
      CI=(0.0D0,1.0D0)
      READ(5,*) A,D,SIGMA
      READ(5,*) T,SMALL
```

```
      WRITE(6,55)A,D,SIGMA,T
C
C  PROGRAM ORIGINALLY WRITTEN WITH SIGMA(2) AND SIGMA(3)
C   INTERCHANGED FROM NOTATION IN PAPER
C
      S=SIGMA(2)
      SIGMA(2)=SIGMA(3)
      SIGMA(3)=S
      A=A*THOU
      D=D*THOU            ! CONVERT FROM KM TO M
      OMEGA=PI*TWO/T
      DO 10 M=1,3
   10    ALPHA(M)=DSQRT(RMU*OMEGA*SIGMA(M))
      calph=cdsqrt(ci)*alpha(1)
      cxpt=-two*d*calph
      cnorm=-omega*ci*(one-cdexp(cxpt))/((one+cdexp(cxpt))*calph)
C     print *,  cnorm
C
C  NY AND NZ : NUMBER OF VALUES OF Y AND Z AT WHICH FIELD IS REQUIRED
C  ARRAY OF FIELD POINTS Y AND Z
C
        READ(5,*) NY,(YY(I),I=1,NY)
        READ(5,*) NZ,(ZZ(J),J=1,NZ)
C                              ! COMPLETE ARRAY (Y(I),Z(J)) NOW READ
C
C  START CALCULATION
C
      DO 1 J=1,NZ
        Z=ZZ(J)*THOU        ! Z COORDINATES IN M
      WRITE (6,52) Z/THOU
      PRINT *,' Z = ',Z
C
C  COMPUTE THROUGH ALL Y VALUES FOR THE GIVEN VALUE OF Z
C
        DO 2 I=1,NY
          F1=.FALSE.
          F2=.FALSE.
         Y=YY(I)*THOU       ! Y COORDINATES IN M
           IF (Y.LE.-A) THEN
             F1=.TRUE.
           ELSE IF (Y.LE.A) THEN
             F2=.TRUE.
           END IF
   20      PRINT *,'          Y = ',Y
           IF(F1.AND.Y.EQ.-A) THEN
             S1=SIGMA(1)
             S2=SIGMA(3)
           END IF
           IF(F2.AND.Y.EQ.A) THEN
             S1=SIGMA(3)
             S2=SIGMA(2)
           END IF
C
C INITIALIZE PARAMETERS
C
           N=0
           CX=C0
           CV=C0
           CW=C0
           FINIS=.FALSE.
```

```
C
C   SUMMATION OF SERIES COMMENCES
C
            DO WHILE (.NOT.FINIS)          ! ADD NEW TERMS TO SERIES
               RK=(2*N+1)*PI/(TWO*D)
         CGAMMA(3)=CDSQRT(RK*RK+CI*ALPHA(3)*ALPHA(3))
               DO 200 M=1,2
         CGAMMA(M)=CDSQRT(RK*RK+CI*ALPHA(M)*ALPHA(M))
                CBETA(M)=CGAMMA(3)*SIGMA(M)/(CGAMMA(M)*SIGMA(3))
  200           CK(M)=TWO*CI*RK*(ALPHA(3)-ALPHA(M))*(ALPHA(3)+ALPHA(M))
     1                 /(D*CGAMMA(M)*CGAMMA(M)*CGAMMA(3)*CGAMMA(3))
               CFACT=CDEXP(-TWO*A*CGAMMA(3))
               CDELTA=(ONE+CBETA(2))*(ONE+CBETA(1))-(ONE-CBETA(2))*
     1                (ONE-CBETA(1))*CFACT*CFACT
               TRIG=DSIN(RK*Z)
               CTRIGV=RK*CGAMMA(3)*DCOS(RK*Z)/(RMU*SIGMA(3))
               CTRIGW=CGAMMA(3)*TRIG/(RMU*SIGMA(3))
C
C   ADJUST CALCULATION ACCORDING TO SEGMENT OF SLAB
C
         IF (F1) THEN     ! CALCULATION FOR LEFT SEGMENT
               CK1=CK(2)
               CK2=CK(1)
               CB1=CBETA(2)
               CB2=CBETA(1)
               CG=CGAMMA(1)
               AL=ALPHA(1)
               CE=CDEXP((Y+A)*CG)
                  CALL SIDE(CK1,CK2,CB1,CB2,CDELTA,CFACT,CG,CE,TRIG,
     1                      CTRIGV,CTRIGW,CTX,CTV,CTW)
             ELSE IF (F2) THEN    ! CALCULATION FOR MIDDLE SEGMENT
               AL=ALPHA(3)
               CG=CGAMMA(3)
               CALL MIDDLE(CK,CBETA,CDELTA,CFACT,CG,TRIG,CTRIGV,
     1                     CTRIGW,CTX,CTV,CTW,Y)
           ELSE       ! CALCULATION FOR RIGHT SEGMENT
               CK1=CK(1)
               CK2=CK(2)
               CB1=CBETA(1)
               CB2=CBETA(2)
               AL=ALPHA(2)
               CG=CGAMMA(2)
               CE=CDEXP((A-Y)*CG)
               CTRIGW = -CTRIGW
                  CALL SIDE(CK1,CK2,CB1,CB2,CDELTA,CFACT,CG,CE,TRIG,
     1                      CTRIGV,CTRIGW,CTX,CTV,CTW)
             END IF
C
C   ACCELERATING SERIES CONVERGENCE AT +A AND -A
C
               IF(ABS(Y).EQ.A) THEN
                 CEXFACT=TWO*CI*OMEGA*DCOS(RK*Z)/(D*RK**2)
                 CTV=CTV-CEXFACT*(S1-S2)/(S1+S2)
               END IF
          CALL SERIES(CX,CV,CW,CTX,CTV,CTW,Z,AL,FINIS,SMALL,N,Y,S1,S2)
               N=N+1
          END DO                          ! SERIES SUMMATION COMPLETE
            YKM=Y/THOU                    ! CONVERT BACK TO KM
            rhoa=(rmu/omega)*(cdabs(cv/cx)**2)
            WRITE (6,53) YKM,CX,CV,CW,rhoa,N
```

```
                IF (F1.AND.Y.EQ.-A) THEN
                  F1=.FALSE.
                  F2=.TRUE.
                  S2=S1
                  S1=SIGMA(3)
                  GO TO 20
                END IF
                IF (F2.AND.Y.EQ.A) THEN
                  F2=.FALSE.
                  S1=S2
                  S2=SIGMA(3)
                  GO TO 20
                END IF
 2      CONTINUE                ! END OF Y DO LOOP
 1     CONTINUE                          ! END OF Z DO LOOP
 52    FORMAT (/,T7,'Z(KM)',T16,'Y(KM)',T35,'BX',T61,'EY',T93,'EZ',
     1         t107,'APP RES',t125,'NO OF',/,F10.3,T29,'REAL      IMAG',
     2           T55,'REAL      IMAG',T87,'REAL      IMAG',
     3           T121,' TERMS IN SUM')
 53    FORMAT (T12,F10.3,T25,2G12.4,T50,2G12.4,
     1             T80,2G12.4,T106,f10.3,T119,I8)
 55    FORMAT ('0 ',10X,'A =',F10.3,' KM',10X,'D =',F10.3,' KM'//
     1         6X,'SIGMA(1) =',F10.6,' S/M',4X,'SIGMA(2) =',F10.6,
     2         ' S/M',4X,'SIGMA(3) =',F10.6,' S/M'//'   T =',F7.1,' SEC')
       END
C
C********************************** SERIES ************************************
      SUBROUTINE SERIES(CX,CV,CW,CTX,CTV,CTW,Z,AL,FINIS,SMALL,N,Y,S1,S2)
C
C   THIS SUBROUTINE SUMS THE SERIES
C
      IMPLICIT    REAL*8 (A,B,D,E,G,H,O-Z),
     1            COMPLEX*16 (C),
     2            LOGICAL*1 (F)
      COMMON      ONE,TWO,CI,A,D,OMEGA,cnorm
C
C   ADD NEXT TERM TO SERIES
C
      CX=CX+CTX
      CV=CV+CTV
      CW=CW+CTW
      TEST=1.DO
      IF (N.GT.2) THEN       ! START TESTING AFTER A FEW TERMS
      IF (CX.NE.O.DO) TX=CDABS(CTX/CX)
      IF (CV.NE.O.DO) TV=CDABS(CTV/CV)
      IF (CW.NE.O.DO) TW=CDABS(CTW/CW)
      TEST=DMAX1(TX,TV,TW)
      END IF
      IF (TEST.GE.SMALL)  RETURN
C   ADD INITIAL TERMS
       FINIS=.TRUE.
         CONST=AL*CDSQRT(CI)
         CDZ=(D-Z)*CONST
         CD=D*CONST
         C1=CDEXP(CDZ)
         C2=ONE/C1
         C3=CDEXP(CD)
         C4=C3+ONE/C3
         CX=CX+(C1+C2)/C4
         IF(ABS(Y).EQ.A) CV=CV+OMEGA*CI*(D-Z)*(S1-S2)/(S1+S2)
```

```
          CV=CV-(OMEGA*CI/CONST)*(C1-C2)/C4
C         cv=cv/cnorm
C         cw=cw/cnorm
          RETURN
          END
C
C
C********************************** SIDE ****************************************
C
          SUBROUTINE SIDE(CK1,CK2,CB1,CB2,CDELTA,CFACT,CG,CE,TRIG,CTRIGV,
         1                CTRIGW,CTX,CTV,CTW)
C   THIS SUBROUTINE CALCULATES THE NEXT TERM IN THE SERIES FOR THE SIDE SEGMENTS
C
          IMPLICIT    REAL*8 (A,B,D,E,G,H,O-Z),
         1            COMPLEX*16 (C)
          COMMON      ONE,TWO,CI,A,D,OMEGA,cnorm
C
C   COMPUTE TERM
C
          CA=(TWO*CK1*CFACT-(ONE+CB1+(ONE-CB1)*CFACT*CFACT)*CK2)/CDELTA
          CTX=CB2*CA*TRIG*CE
          CTV=CA*CTRIGV*CE/CG
          CTW=-CA*CTRIGW*CE
          END
C
C
C************************** MIDDLE ****************************************
C
          SUBROUTINE MIDDLE(CK,CB,CD,CF,CG,TRIG,CTRIGV,CTRIGW,CTX,CTV,CTW,Y)
C
C   THIS SUBROUTINE CALCULATES THE NEXT TERM IN THE SERIES FOR THE MIDDLE SEGMENT
C
          IMPLICIT     REAL*8 (A,B,D,E,G,H,O-Z),
         1           COMPLEX*16 (C)
          COMPLEX*16  CK(2),CB(2)
          COMMON      ONE,TWO,CI,A,D,OMEGA,cnorm
C
C   COMPUTE TERM
C
          C1=((ONE+CB(1))*CK(2)-(ONE-CB(2))*CK(1)*CF)/CD
          C2=((ONE+CB(2))*CK(1)-(ONE-CB(1))*CK(2)*CF)/CD
          CL=C1*CDEXP((Y-A)*CG)
          CR=C2*CDEXP(-(Y+A)*CG)
          CTX=TRIG*(CL+CR)
          CTV=(CL+CR)*CTRIGV/CG
          CTW=CTRIGW*(CR-CL)
          END
```

```
      PROGRAM BVOL
C
C  ************************** MAIN ************************************
C    A B-POLARIZATION CALCULATION IN ELECTROMAGNETIC INDUCTION
C  THIS PROGRAM COMPUTES THE VOLTAGES AT THE SURFACE OF A
C  SEGMENTED CONDUCTING SLAB DUE TO A UNIFORM HORIZONTAL MAGNETIC FIELD.
C  THE MODEL CONSISTS OF A SLAB OF THICKNESS "D" UNDERLAIN BY A PERFECT
C  CONDUCTOR AT DEPTH Z=D.  THE SLAB IS DIVIDED INTO 3 SEGMENTS :
C       (1) Y.LT.-A OF CONDUCTIVITY SIGMA(1) .
C       (2) Y BETWEEN -A AND A OF CONDUCTIVITY SIGMA(2).
C       (3) Y.GT.+A OF CONDUCTIVITY SIGMA(3).
C  THE INDUCING MAGNETIC FIELD IS UNIFORM IN THE X-DIRECTION AND HAS
C  A PERIOD "T" SPECIFIED BY THE USER.  VACUUM PERMEABILITY IS ASSUMED
C  EVERYWHERE.
C
C  INPUT DATA TO BE PROVIDED BY THE USER SHOULD BE IN FREE FORMAT IN
C  FOR005 : (1) A : HALF-WIDTH IN KM OF THE MIDDLE SEGMENT.
C           (2) D : THICKNESS OF THE SLAB IN KM.
C           (3) SIGMA(3) : ARRAY CONTAINING CONDUCTIVITY VALUES IN S/M
C           (4) T : PERIOD OF FIELD, IN SECONDS.
C           (5) SMALL : CONTROL PARAMETER FOR ACCURACY.
C           (6) NY AND YY : THE NUMBER OF HORIZONTAL POINTS Y AT WHICH
C                           THE FIELD IS REQUIRED, AND THEIR COORDINATES
C           (7) NZ AND ZZ : THE NUMBER OF VERTICAL POINTS Z AND
C                           THEIR COORDINATES
C  THE CONTROL PARAMETER "SMALL" MAY BE CHANGED TO PROVIDE QUICKER
C  (LESS ACCURATE) CALCULATIONS.  NORMALLY SMALL = 1.0D-8
C  RESULTS ARE WRITTEN TO FOR006
C  SUBROUTINES USED : SERIES  -  SIDE  -  MIDDLE
C
C  DEFINE VARIABLE TYPES
C
      IMPLICIT     REAL*8 (A,B,D,E,G,H,O-Z),
     1             COMPLEX*16 (C),
     2             LOGICAL*1 (F)
      COMPLEX*16 CGAMMA(3),CBETA(2),CK(2),CVOL(200)
      REAL*8       YY(200),ZZ(50),SIGMA(3),ALPHA(3)
      INTEGER      NM(200)
      COMMON       ONE,TWO,CI,A,D,OMEGA
C
C  DEFINE CONSTANTS
C
      PARAMETER (THOU=1.0D3,PI=3.141592653589793238)
      PARAMETER (RMU=PI*4.0D-7,CO=(0.0D0,0.0D0))
C
C  MODEL PARAMETERS
C
      ONE=1.0D0
      TWO=2.0D0
      CI=(0.0D0,1.0D0)
      READ(5,*) A,D,SIGMA
      READ(5,*) T,SMALL
      WRITE(6,55)A,D,SIGMA,T
C
C  PROGRAM ORIGINALLY WRITTEN WITH SIGMA(2) AND SIGMA(3)
C   INTERCHANGED FROM NOTATION IN PAPER
C
      S=SIGMA(2)
      SIGMA(2)=SIGMA(3)
      SIGMA(3)=S
```

```
      A=A*THOU
      D=D*THOU            ! CONVERT FROM KM TO M
      OMEGA=PI*TWO/T
      DO 10 M=1,3
   10    ALPHA(M)=DSQRT(RMU*OMEGA*SIGMA(M))
C
C  NY AND NZ : NUMBER OF VALUES OF Y AND Z AT WHICH FIELD IS REQUIRED
C  ARRAY OF FIELD POINTS Y AND Z
C
        READ(5,*) NY,(YY(I),I=1,NY)
        READ(5,*) NZ,(ZZ(J),J=1,NZ)
C                              ! COMPLETE ARRAY (Y(I),Z(J)) NOW READ
C
C  START CALCULATION
C
      DO 1 J=1,NZ
        Z=ZZ(J)*THOU          ! Z COORDINATES IN M
        WRITE (6,52) Z/THOU
        PRINT *,' Z = ',Z
C
C  COMPUTE THROUGH ALL Y VALUES FOR THE GIVEN VALUE OF Z
C
        DO 2 I=1,NY
          F1=.FALSE.
          F2=.FALSE.
          Y=YY(I)*THOU        ! Y COORDINATES IN M
           IF (Y.LE.-A) THEN
             F1=.TRUE.
           ELSE IF (Y.LE.A) THEN
             F2=.TRUE.
           END IF
  20       PRINT *,'          Y = ',Y
C
C INITIALIZE PARAMETERS
C
          N=0
          CVL=C0
          FINIS=.FALSE.
C
C  SUMMATION OF SERIES COMMENCES
C
          DO WHILE (.NOT.FINIS)          ! ADD NEW TERMS TO SERIES
            RK=(2*N+1)*PI/(TWO*D)
            CGAMMA(3)=CDSQRT(RK*RK+CI*ALPHA(3)*ALPHA(3))
            DO 200 M=1,2
              CGAMMA(M)=CDSQRT(RK*RK+CI*ALPHA(M)*ALPHA(M))
              CBETA(M)=CGAMMA(3)*SIGMA(M)/(CGAMMA(M)*SIGMA(3))
  200         CK(M)=TWO*CI*RK*(ALPHA(3)-ALPHA(M))*(ALPHA(3)+ALPHA(M))
     1              /(D*CGAMMA(M)*CGAMMA(M)*CGAMMA(3)*CGAMMA(3))
              CFACT=CDEXP(-TWO*A*CGAMMA(3))
              CDELTA=(ONE+CBETA(2))*(ONE+CBETA(1))-(ONE-CBETA(2))*
     1              (ONE-CBETA(1))*CFACT*CFACT
              CTRIG=RK*CGAMMA(3)*DCOS(RK*Z)/(RMU*SIGMA(3))
C
C  ADJUST CALCULATION ACCORDING TO SEGMENT OF SLAB
C
              IF (F1) THEN     ! CALCULATION FOR LEFT SEGMENT
                   CK1=CK(2)
                   CK2=CK(1)
                   CB1=CBETA(2)
```

```
                    CB2=CBETA(1)
                    CG=CGAMMA(1)
                    AL=ALPHA(1)
                    CE=CDEXP((Y+A)*CG)
                  CALL SIDE(CK1,CK2,CB1,CB2,CDELTA,CFACT,CG,CE,CTRIG,CTVL)
                ELSE IF (F2) THEN    ! CALCULATION FOR MIDDLE SEGMENT
                  AL=ALPHA(3)
                  CG=CGAMMA(3)
                  CALL MIDDLE(CK,CBETA,CDELTA,CFACT,CG,CTRIG,CTVL,Y)
                ELSE       ! CALCULATION FOR RIGHT SEGMENT
                    CK1=CK(1)
                    CK2=CK(2)
                    CB1=CBETA(1)
                    CB2=CBETA(2)
                    AL=ALPHA(2)
                    CG=CGAMMA(2)
                    CE=CDEXP((A-Y)*CG)
                  CALL SIDE(CK1,CK2,CB1,CB2,CDELTA,CFACT,CG,CE,CTRIG,CTVL)
                  CTVL=-CTVL
                 END IF
C
C    SUMMING THE SERIES
C
              CALL SERIES(CVL,CTVL,Z,AL,FINIS,SMALL,N,Y)
              N=N+1
            END DO                          ! SERIES SUMMATION COMPLETE
              IF(Y.EQ.-A) THEN
                IF (F1) THEN
                  F1=.FALSE.
                  F2=.TRUE.
                  K=I
                  NM(I)=N
                  CVOL(I)=CVL
                  GOTO 20
                ELSE
                  NORM=N
                  CNORM=CVL
                  GOTO 2
                END IF
              END IF
              IF(Y.EQ.A) THEN
                IF (F2) THEN
                  F2=.FALSE.
                  NORP=N
                  CNORP=CVL
                  GOTO 20
                ELSE
                  L=I
                  CVOLL=CVL
                END IF
              END IF
            NM(I)=N
            CVOL(I)=CVL
2       CONTINUE                          ! END OF Y DO LOOP
        DO 3 I=1,NY
          IF(I.LE.K) CVOL(I)=CVOL(I)-CVOL(K)+CNORM
          IF(I.GE.L) CVOL(I)=CVOL(I)-CVOLL+CNORP
          IF(I.EQ.L) WRITE (6,53) YY(L),CNORP,NORP
          WRITE (6,53) YY(I),CVOL(I),NM(I)
3         IF(I.EQ.K) WRITE (6,53) YY(K),CNORM,NORM
```

```
  1     CONTINUE                          ! END OF Z DO LOOP
  52    FORMAT (/, T7, 'Z(KM)', T16, 'Y(KM)', T36, 'VOLTAGE (mV/nT)',
       1          /, F10.3, T34, ' REAL           IMAG',
       2          T66, 'NO OF TERMS IN SUM')
  53    FORMAT (T12, F10.3, T30, 2G14.6, T66, I8)
  55    FORMAT ('0 ', 10X, 'A =', F10.3, ' KM', 10X, 'D =', F10.3, ' KM'//
       1        6X, 'SIGMA(1) =', F10.6, ' S/M', 4X, 'SIGMA(2) =', F10.6,
       2        ' S/M', 4X, 'SIGMA(3) =', F10.6, ' S/M'//'  T =', F7.1, ' SEC')
        END
C
C********************************* SERIES ************************************
      SUBROUTINE SERIES(CVL, CTVL, Z, AL, FINIS, SMALL, N, Y)
C
C   THIS SUBROUTINE SUMS THE SERIES
C
      IMPLICIT   REAL*8 (A, B, D, E, G, H, O-Z),
     1           COMPLEX*16 (C),
     2           LOGICAL*1 (F)
      COMMON     ONE, TWO, CI, A, D, OMEGA
C
C   ADD NEXT TERM TO SERIES
C
      CVL=CVL+CTVL
      TV=1.DO
        IF (N.GT.2) THEN       ! START TESTING AFTER A FEW TERMS
        IF (CVL.NE.0.DO) TV=CDABS(CTVL/CVL)
        END IF
      IF (Y.EQ.0) TV=0.DO
      IF (TV.GE.SMALL)  RETURN
C   ADD INITIAL TERMS
        FINIS=.TRUE.
        CONST=AL*CDSQRT(CI)
        CDZ=(D-Z)*CONST
        CD=D*CONST
        C1=CDEXP(CDZ)
        C2=ONE/C1
        C3=CDEXP(CD)
        C4=C3+ONE/C3
        CVL=CVL-Y*(OMEGA*CI/CONST)*(C1-C2)/C4
        CVL=CVL*1.E-6
      RETURN
      END
C
C
C********************************* SIDE **************************************
C
      SUBROUTINE SIDE(CK1, CK2, CB1, CB2, CDELTA, CFACT, CG, CE, CTRIG, CTVL)
C
C   THIS SUBROUTINE CALCULATES THE NEXT TERM IN THE SERIES FOR THE SIDE SEGMENTS
C
      IMPLICIT   REAL*8 (A, B, D, E, G, H, O-Z),
     1           COMPLEX*16 (C)
      COMMON     ONE, TWO, CI, A, D, OMEGA
C
C   COMPUTE TERM
C
      CA=(TWO*CK1*CFACT-(ONE+CB1+(ONE-CB1)*CFACT*CFACT)*CK2)/CDELTA
      CTVL=CE*CA*CTRIG/(CG**TWO)
      END
C
```

```
C
C************************** MIDDLE ****************************************
C
      SUBROUTINE MIDDLE(CK,CB,CD,CF,CG,CTRIG,CTVL,Y)
C
C   THIS SUBROUTINE CALCULATES THE NEXT TERM IN THE SERIES FOR THE MIDDLE SEGMEN
C
      IMPLICIT     REAL*8 (A,B,D,E,G,H,O-Z),
     1           COMPLEX*16 (C)
      COMPLEX*16  CK(2),CB(2)
      COMMON      ONE,TWO,CI,A,D,OMEGA
C
C   COMPUTE TERM
C
      C1=((ONE+CB(1))*CK(2)-(ONE-CB(2))*CK(1)*CF)/CD
      C2=((ONE+CB(2))*CK(1)-(ONE-CB(1))*CK(2)*CF)/CD
      CL=C1*(CDEXP((Y-A)*CG)-CDEXP(-A*CG))
      CR=C2*(CDEXP(-(Y+A)*CG)-CDEXP(-A*CG))
      CTVL=(CL-CR)*CTRIG/(CG**TWO)
      END
```

```
      SUBROUTINE VOLT(FIELD,DERIV,RES,RESNO,ROW,YGRID)
C     --------a special execution routine.  Called by "SPEC1"
C     --- flag = 0.....ie: E field at left side of boundary used
      IMPLICIT REAL*8 (A-H,O-Z)
      INCLUDE 'INCLIB:CPROG.INC'
      INCLUDE 'INCLIB:FORSYS.INC'
      COMMON /CGEN/ PI,OMEGA,RMU0,PRFECT,RINSUL
      COMMON /LOOP/ IX1,IX2,IXD,IY1,IY2,IYD,IZ1,IZ2,IZD
      COMPLEX*16 DERIV(ncptd,nxe,nye,nze),TERMI,TERMJ,TERML
     1,VNORM,CI,VLT(100)
      REAL*8  RES(nr1,nres),VLTRE,VLTIM,YGRID(ny),EREA,EIMA
      INTEGER*4  RESNO(nyc,nrows),ROW(nxc,nzc)
      CHARACTER*35  HEAD,HEAD2
      HEAD='REAL AND IMAGINARY VOLTAGES (mV/nT)'
      HEAD2='REAL AND IMAGINARY ELECTRIC FIELDS '
      WRITE(7,98) HEAD2
      WRITE(9,99) HEAD
   98 FORMAT(///,21X,A35//,7X,'Y(KM)',13X,'REAL E',21X,'IMAG E'/)
   99 FORMAT(///,21X,A35//,7X,'Y(KM)',13X,'REAL V',21X,'IMAG V'/)
      CON=OMEGA*RMU0
      CI=(0.D0,1.D0)
      VLT(3)=(0.D0,0.D0)
      DO 20 IY=4,IY2
            M=IY-3
            I=IY-2
            J=IY-1
            L=IY
            RM=RES(1,RESNO(M,ROW(IX1,1)))/CON
            RI=RES(1,RESNO(I,ROW(IX1,1)))/CON
            RJ=RES(1,RESNO(J,ROW(IX1,1)))/CON
            RL=RES(1,RESNO(L,ROW(IX1,1)))/CON
            hm=YGRID(L)-YGRID(J)
            hm1=YGRID(J)-YGRID(I)
            hsum=hm+hm1
            RJGR=(hm1*RI+hm*RJ)/hsum
            FACT=(RJ*hm**2)/(6*RJGR*hsum)
            TERMI=hm*RI*DERIV(1,1,I,1)/(hm1*RM)
            TERML=(2+3*hm1*RI/(RJ*hm))*DERIV(1,1,L,1)
            TERMJ=(4*RJ/RI+(3*hm1/hm+hm/hm1)+CI*hm*hm1*
     1           (RJ/RI-1)/(2*RJ))*DERIV(1,1,J,1)
            VLT(L)=VLT(J)+FACT*(TERMJ+TERML-TERMI)
            IF(YGRID(L).EQ.0.0)VNORM=VLT(L)
   20 CONTINUE
      IY11=4
      IF(IY1 GE.4) IY11=IY1
      DO 40 L=IY11,IY2
         VLT(L)=VLT(L)-VNORM
         VLTRE=DREAL(VLT(L))*(1D-6)
         VLTIM=DIMAG(VLT(L))*(1D-6)
         YG=YGRID(L)/1000
         EREA=DREAL(DERIV(1,1,L,1))
         EIMA=DIMAG(DERIV(1,1,L,1))
         WRITE(7,100)YG,EREA,EIMA
         WRITE(9,100)YG,VLTRE,VLTIM
  100    FORMAT(5X,F11.5,5X,2(D23.15,5X))
   40 CONTINUE
C
C *** END OF DATA FLAG FOR USE IN VOLTAGE DIFFERENCE CALCULATION ***
C
      YG=5000
```

```
VLTRE=0.00
VLTIM=0.00
WRITE(9,100)YG,VLTRE,VLTIM
RETURN
END
```

```
      SUBROUTINE VOLT(FIELD,DERIV,RES,RESNO,ROW,YGRID)
C     --------a special execution routine  Called by "SPEC1"
C     ----flag = 1.....  ie: E field at right side of boundary used
      IMPLICIT REAL*8 (A-H,O-Z)
      INCLUDE 'INCLIB:CPROG.INC'
      INCLUDE 'INCLIB:FORSYS.INC'
      COMMON /CGEN/ PI,OMEGA,RMUO
      COMMON /LOOP/ IX1,IX2,IXD,IY1,IY2,IYD,IZ1,IZ2,IZD
      COMPLEX*16 DERIV(ncptd,nxe,nye,nze),TERMI,TERMJ,TERML
     1,VNORM,CI,VLT(100)
      REAL*8  RES(nr1,nres),VLTRE,VLTIM,YGRID(ny),RMAG,PANG,EREA,EIMA
      INTEGER*4  RESNO(nyc,nrows),ROW(nxc,nzc)
      CHARACTER*35  HEAD,HEAD2
      HEAD='REAL AND IMAGINARY VOLTAGES (mV/m)'
      HEAD2='REAL AND IMAGINARY ELECTRIC FIELDS '
      PER=2*PI/OMEGA
      WRITE(7,98) PER,HEAD2
      WRITE(9,99) PER,HEAD
   98 FORMAT(/,5X,'T=',F9.3,'s',4X,A35/,7X,'Y(KM)',13X,'REAL E',21X,
     1'IMAG E'/)
   99 FORMAT(/,5X,'T=',F9.3,'s',4X,A35/,7X,'Y(KM)',13X,'REAL V',21X,
     1'IMAG V'/)
      CON=OMEGA*RMUO
      CI=(0.D0,1.D0)
      VLT(2)=(0.D0,0.D0)
      DO 20 IY=3,IY2
            I=IY-2
            J=IY-1
            L=IY
            RI=RES(1,RESNO(1,ROW(IX1,1)))/CON
            RJ=RES(1,RESNO(J,ROW(IX1,1)))/CON
            RL=RES(1,RESNO(L,ROW(IX1,1)))/CON
            hm=YGRID(L)-YGRID(J)
            hm1=YGRID(J)-YGRID(I)
            hsum=hm+hm1
            RJGR=(hm1*RI+hm*RJ)/hsum
            FACT=(RJ*hm**2)/(6*RJGR*hsum)
            TERMI=hm*DERIV(1,1,I,1)/hm1
            TERML=(2*RJ/RL+3*hm1*RI/(RL*hm))*DERIV(1,1,L,1)
            TERMJ=(4+(3*hm1/hm+hm/hm1)*RI/RJ+CI*hm*hm1*
     1           (1-RI/RJ)/(2*RJ))*DERIV(1,1,J,1)
            VLT(L)=VLT(J)+FACT*(TERMJ+TERML-TERMI)
            IF (YGRID(L).EQ.0.0) VNORM=VLT(L)
   20 CONTINUE
      IY11=3
      IF(IY1.GE.3) IY11=IY1
      DO 40 L=IY11,IY2
            VLT(L)=VLT(L)-VNORM
            VLTRE=DREAL(VLT(L))*(1D-6)
            VLTIM=DIMAG(VLT(L))*(1D-6)
            YG=YGRID(L)/1000
            EREA=DREAL(DERIV(1,1,L,1))
            EIMA=DIMAG(DERIV(1,1,L,1))
            WRITE(7,100)YG,EREA,EIMA
            WRITE(9,100)YG,VLTRE,VLTIM
  100       FORMAT(5X,F11.5,5X,2(D23.15,5X))
   40 CONTINUE
C
C *** END OF FILE FLAG USED IN VOLTAGE DIFFERENCE CALCULATION ***
C
```

```
YG=5000
VLTRE=0.00
VLTIM=0.00
WRITE(9,100)YG,VLTRE,VLTIM
RETURN
END
```

```
C ****************  PROGRAM VDIFE  ******************
C
C  CALCULATES THE VOLTAGE              ELECTRIC FIELD
C  PERPENDICULAR AND PARALLEL TO A STRIKE WHEN THE
C  ANGLE BETWEEN THE ELECTRODE PROFILE AND THE
C  STRIKE IS <35 degrees
C
C*****************************************************
      IMPLICIT REAL*8 (A-H,O-Z)
      REAL*8 y(100),vr(100),vi(100),yc(100),yd(100),yv(100)
     1,yn(100),ye(100),ERY(100),EIY(100),ERX(100),EIX(100)
      COMPLEX*16 EV,EU,VV,VD(200),VC(200),vdiff,vddiff,EY(100)
     1,EX(100),EXX(100),B,E,r
      CHARACTER  HEAD1*28,HEAD2*45,HEAD3*45,HEAD4*45,ERROR*20
      read(9,100) per
      read(12,100) per
  100 FORMAT(/,7x,F9.3//)
      HEAD1='ANGLE BETWEEN Y AND STRIKE??'
      HEAD2='E FIELDS PERPENDICULAR AND PARALLEL TO STRIKE'
      HEAD3='ORIGINAL FIELD  (perpendicular to the strike)'
      HEAD4='   ELECTRIC FIELD FROM VOLTAGE DIFFERENCES    '
      ERROR='GRID POINT NOT FOUND'
      WRITE(6,101) HEAD1
      READ(5,*) ANG
      SI=SIND(ANG)
      CO=COSD(ANG)
      WRITE(10,102) HEAD2,per,ANG
      WRITE(11,104) HEAD3,per,ANG
      WRITE(13,104) HEAD4,per,ANG
  102 FORMAT(///,20X,A45/,30X,'T=',F7.3,'s',4X,'angle=',F7.2,'deg'/
     1,7X,6H X'(m),18X,'E (y-dirtn) mV/km',29X,'E (x-dirtn) mV/km'/)
  104 FORMAT(///,20X,A45/,30X,'T=',F7.3,'s',4X,'angle=',F7.2,'deg'/
     1,7X,6H X'(m),18X,'E (y-dirtn) mV/km'/)
  103 FORMAT(//,10X,A20,5x,F9.5/)
  101 FORMAT(//,10X,A28,2x)
      pi=3.14159
      omega=2*pi/per
      rmu0=4e-07*pi
      B=cmplx(1.D0,0.D0)
      A1=rmu0/omega
      A2=180.D0/pi
      do 10 i=1,200
        read(9,*) YV(i),VR(i),VI(i)
        if(YV(i).eq.5000.and.VR(i).eq.VI(i)) goto 20
        read(12,*) YE(i),ERY(i),EIY(i)
   10 continue
   20 jum=i-1
      read(7,*) num,ydd
C  ***    CHANGING TO km FOR CALCULATION  ***
      ydd=ydd/1000
      do 50 i=1,num
      read (7,*) YN(i)
      Y(i)=YN(i)/1000
      YC(i)=Y(i)*SI
      YD(i)=YC(i)-ydd*CO
      l=0
      ll=0
      do 42 j=1,jum
        CHK1=ABS(YV(j)-YC(i))
         if(CHK1.le.0.00001) then
```

```
            VC(i)=cmplx(VR(j),VI(j))
            EY(i)=cmplx(ERY(j),EIY(j))/1000
            l=l+1
          end if
         CHK2=ABS(YV(j)-YD(i))
          if(CHK2.le.0.00001) then
            VD(i)=cmplx(VR(j),VI(j))
            ll=ll+1
          end if
          if(l.eq.1.and.ll.eq.1) GOTO 50
          if(YV(j).gt.YC(i).and.YV(j).gt.YD(i)) then
            if(ll.eq.0) write(6,103) ERROR,YD(i)
            if(l.eq.0)  write(6,103) ERROR,YC(i)
            num=i
            goto 55
          end if
   42 continue
   50 continue
   55 do 60 i=1,num
C    ***  CALCULATING THE VOLTAGE DIFFERENCE V AND U  ***
C    ***  PERPENDICULAR AND PARALLEL TO THE STRIKE    ***
          ydiff=(Y(i+1)-Y(i))
          vdiff=(VC(i+1)-VC(i))/ydiff
          vddiff=(VD(i)-VC(i))/ydd
          EV=vdiff*SI-vddiff*CO
          EU=-vdiff*CO-vddiff*SI
          VV=vdiff/SI
          E=1000*EV
         CALL APRES(E,B,A1,A2,RESM1,PHANG)
         WRITE(10,105) YN(i),EV,EU
         WRITE(11,106) YN(i),EY(i)
         WRITE(13,106) YN(i),VV
         WRITE(14,105) YN(i),E,resm1,phang
  105    FORMAT(5X,F9.3,5X,4(D18.10,5X))
  106    FORMAT(5X,F9.3,5X,2(D18.10,5X))
   60    continue
         stop
         end
         SUBROUTINE APRES(E,B,A1,A2,RESM1,PHANG)
         IMPLICIT REAL*8 (A-H,O-Z)
         real*8 resm1,phang,A1,A2
         complex*16 B,E,r
            if (e .eq. cmplx(0.d0,0.d0)) then
              resm1 = 0.d0
              phang = 0.d0
            else
              if (abs(b).ge.1.d-20) then
                 r = -e/b
                 resm1 = a1 * abs(r)*abs(r)
                 r1 = dimag(r)
                 r2 = dreal(r)
                 r3 = r1 / r2
                 if (abs(r3).lt.1.d30) then
                    phang = a2 * atan( r3 )
                 else    !avoid zero divide
                    phang = 90.d0
                 end if
              else    !avoid zero divide
                 resm1 = 1.d20
                 phang = 0.d0
```

```
    end if
end if
return
END
```

VITA

Surname: Poll Given Names: Helena Eva

Place of Birth: Toronto, Ontario Date of Birth: Oct. 18, 1962

Educational Institutions Attended, with Dates of Entering and Leaving:

UNIVERSITY OF GUELPH, ONTARIO 1981 TO 1985

UNIVERSITY OF VICTORIA, B.C. 1985 TO 1987

Degrees, Diplomas, Etc., Awarded, with Dates and Names of Institutions:

B.Sc. (Honors) 1985 University of Guelph, Ontario

Honors and Awards

University of Guelph Entrance Scholarship 1981
University of Guelph Physics Scholarship 1981-1982

Publications

Calculations of Voltages for Magneto-telluric Modelling of a Region with Near-Surface Inhomogeneities. PEPI, (submitted)

PARTIAL COPYRIGHT LICENSE

I hereby grant the right to lend my thesis (the title of which is shown below) to users of the University of Victoria Library, and to make *single copies only* for such users or in response to a request from the Library of any other university, or similar institution, on its behalf or for one of its users. I further agree that permission for extensive copying of this thesis for scholarly purposes may be granted by me or a member of the University designated by me. It is understood that copying or publication of this thesis for financial gain shall not be allowed without my written permission.

Title of Thesis

CALCULATIONS OF VOLTAGES FOR MAGNETO-TELLURIC MODELLING OF A REGION WITH NEAR-SURFACE INHOMOGENEITIES

Author [redacted]

Signature

HELENA EVA POLL

Name

April 1987

Date